Palaeogeography, Palaeoclimatology, Palaeoecology xxx (xxxx) xxx

Contents lists available at ScienceDirect

Palaeogeography, Palaeoclimatology, Palaeoecology

journal homepage: www.elsevier.com/locate/palaeo

Last deglaciation flooding events in the Southern Carpathians as revealed by the study of cave deposits from Muierilor Cave, Romania

Ionuț-Cornel Mirea [a,i,j,1], Marius Robu [b,*,1], Alexandru Petculescu [a,j], Marius Kenesz [c,j], Luchiana Faur [b,j], Răzvan Arghir [a,j], Viorica Tecsa [d,e], Alida Timar-Gabor [d,e], Relu-Dumitru Roban [f], Cristian G. Panaiotu [g], Arash Sharifi [h], Ali Pourmand [h], Vlad A. Codrea [i], Silviu Constantin [a,j,k,*,1]

[a] "Emil Racoviță" Institute of Speleology, Center for Geochronology and Paleoclimate, Frumoasă 31, 010986, Bucharest, Romania
[b] "Emil Racoviță" Institute of Speleology, Romanian Academy, Calea 13 Septembrie 13, 050711, Bucharest, Romania
[c] "Emil Racoviță" Institute of Speleology, Cluj Branch, Clinicilor 5, 400006, Cluj-Napoca, Romania
[d] Interdisciplinary Research Institute on Bio-Nano-Science of Babeș- Bolyai University, Treboniu Laurean 42, 400271 Cluj-Napoca, Romania
[e] Faculty of Environmental Sciences and Engineering, Babeș- Bolyai University, Fântânele 30, 400294 Cluj-Napoca, Romania
[f] Faculty of Geology and Geophysics, University of Bucharest, Lithos Reserch Center, Nicolae Bălcescu 1, 010041 Bucharest, Romania
[g] Faculty of Physics, University of Bucharest, Paleomagnetic Laboratory, Atomiștilor 405, 077125 Măgurele, Romania
[h] Neptune Isotope Laboratory, Division of Marine Geology and Geophysics, University of Miami, RSMAS, 4600 Rickenbacker Causeway, Miami, FL 33149, USA
[i] Laboratory of Paleotheriology and Quaternary Geology, Faculty of Biology - Geology, Babeș- Bolyai University, Kogălniceanu Street 1, 400084, Cluj-Napoca, Romania
[j] Romanian Institute of Science and Technology, Virgil Fulicea 3, 400022 Cluj-Napoca, Romania
[k] Centro Nacional de Investigación sobre la Evolución Humana, CENIEH, Paseo de Atapuerca s/n, 09002, Burgos, Spain

ARTICLE INFO

Keywords:
Cave bears
Cave genesis
MIS 3–2 fauna
LGM
Romanian Carpathians

ABSTRACT

Caves often hold valuable palaeoclimate archives including speleothems, fossil remains, and clastic sediments that complement each other. This paper presents a multi-archive interdisciplinary study of an extensive deposit of fossil mammals from the scientific reserve in the Muierilor Cave, Southern Carpathians, Romania. We present two new palaeontological excavations that indicate a high abundance and diversity of MIS 3–2 fossil mammals (carnivores, omnivores and herbivores) synchronous with the early modern humans known from this cave. Using geochronological and sedimentological methods, we present a general reconstruction of the cave evolution between ~120 kyr B.P. and the Holocene. The study is based on a combination of geochronological tools including OSL dating of sediments, U/Th dating of speleothems, and radiocarbon dating of fossil remains, with a total of 54 ages. Based on U/Th dating of speleothems from stratigraphically-relevant positions, we show that the MIS 3 assemblage of fossil mammals were massively reworked and deposited during the post-LGM deglaciation, slightly earlier than previously known for the Southern Carpathians. On the other hand, several young radiocarbon ages of cave bear samples suggest that the Southern Carpathians might have been functioning as a glacial refuge for this species as late as ~22 kyr B.P.

1. Introduction

Studies investigating cave deposits are increasingly becoming more relevant due to the value of the palaeoenvironmental archives they hold (Sasowsky and Mylorie 2007; Ford and Williams 2013; Bradley 2015). Karst archives include vertebrate remains, sediments, speleothems, and invertebrate fossil assemblages (Moldovan et al. 2016; Winkler et al. 2016; Lyman 2017; Hatvani et al. 2018). These can be investigated through the use of various proxies and dating techniques that reveal stages of cave evolution connected to regional or global events.

The systematic study of cave deposits allows for a better understanding of the evolution of palaeoenvironment at both local and regional scale and for restraining the main evolutionary stages using absolute dating techniques (Fairchild and Baker 2012; Constantin et al. 2014; Álvarez-Lao et al. 2015). Large mammal assemblages and micromammals are some of the oldest palaeontological records (Lyman

* Corresponding authors.
E-mail addresses: marius.robu@iser.ro (M. Robu), silviu.constantin@iser.ro (S. Constantin).
[1] These authors had an equal contribution.

https://doi.org/10.1016/j.palaeo.2020.110084
Received 2 March 2020; Received in revised form 1 October 2020; Accepted 11 October 2020
Available online 22 October 2020

1994; Parmalee 2005) to indirectly determine the ages of cave sediments and the general climatic conditions for a particular region. Speleothems are the most used climatic archives in caves due to the potential for palaeoclimate reconstructions at regional scale that which can be accurately dated by using the U/Th method (McDermott 2004; Fairchild et al. 2006; Obreht et al. 2017; Hatvani et al. 2018; Rossi et al. 2018; Isola et al. 2019). Clastic sediments found in caves are an important archive on the dynamics of the palaeohydrology of the underground settings (Sun et al. 2017; Arriolabengoa et al. 2018). Overall, cave deposits are a valuable source of information in tracing past climatic features, especially the deposits from the temperate environments (Constantin et al. 2014). Cave deposits can be affected by post-depositional alteration (palaeohydrological events, sediment compression, trampling, rock-fall; Sasowsky and Mylorie 2007) and reworking processes (e.g. floods). Most floods can be linked with extreme precipitation, snow and ice melting (White 2007), the latter being related with the deglaciation pulses (Ballesteros et al. 2019).

For the Romanian Carpathians, only a few studies on the timing of the last deglaciation and the magnitude of related processes have been published (e.g. Urdea 2004; Reuther et al. 2007; Urdea and Reuther 2009; Urdea et al. 2011; Kuhlemann et al. 2013; Gheorghiu et al. 2015). A higher number of interdisciplinary studies of cave deposits were carried out in some of the most important karstic systems of the Romanian Carpathians to help establish a broader palaeoenvironmental and palaeoclimatic framework (Onac et al. 2002; Constantin, 2003; Constantin et al., 2006; 2007; 2014; Tămaş et al. 2005; Panaiotu et al. 2013; Drăguşin et al., 2014; Robu 2015; Moldovan et al. 2016; Tîrlă et al. 2020).

The Southern Carpathians host sites with extensive cave deposits (speleothems, sediments and fossil remains) of high importance both as palaeoclimate archives and as repositories of anatomically modern humans remains (Riel-Salvatore et al. 2008; Häuselmann et al. 2010; Doboş et al. 2010; Fu et al. 2015, 2016). Muierilor Cave holds an impressive Marine Isotope Stage 3 (MIS 3) fossil assemblage (Doboş et al. 2010) as well as sedimentological and mineralogical features relevant for the regional geological evolution during the Quaternary (Diaconu et al., 2008). Since the late 1950s, comprehensive research on Muierilor Cave has been carried out on geomorphology (Ion and Lupu 1962), bat fauna (Dumitrescu et al. 1963), palaeontology (Bombiță 1954), geology and mineralogy (Diaconu and Medeşan 1975; Diaconu et al., 2008) and palaeoanthroplogy (Doboş et al. 2010). Hence, the valuable inventory found in the Muierilor Cave makes it a suitable site for interdisciplinary research.

In this paper, we report new data on the palaeontological and sedimentological context and propose a scenario for the evolution of the Muierilor cave system that broadly spans over the last ~120,000 years. We carried out an interdisciplinary study by analyzing absolutely dated clastic sediments, speleothems, and fossil remains, complementary to the palaeontological study of two new excavations.

2. The site

2.1. Geological setting

The studied area is located in the southeastern part of the Parâng Mountains (Southern Carpathians). It includes a basement of

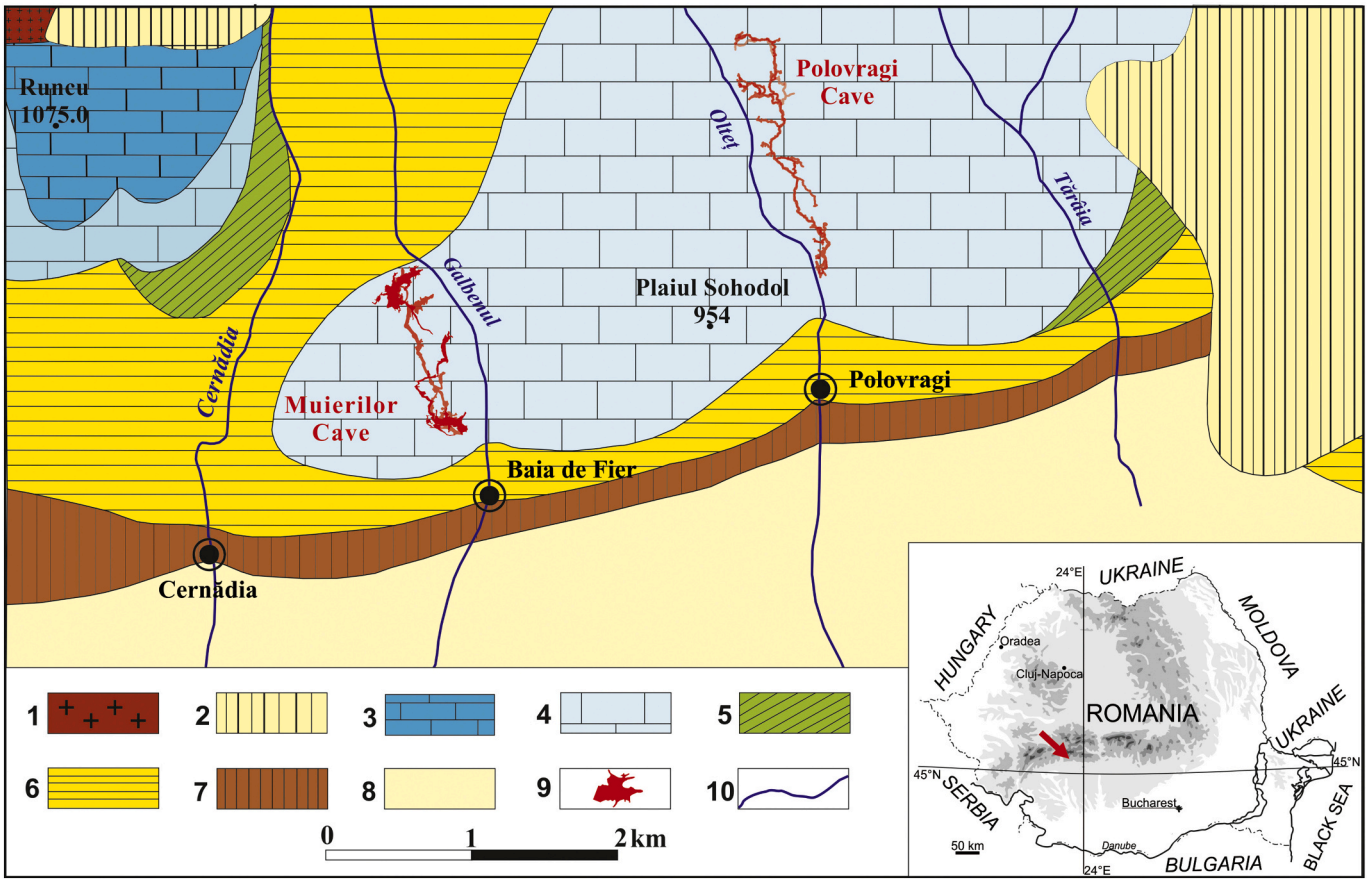

Fig. 1. Geological map of the Polovragi - Cernădia area (modified after Diaconu et al., 2008). 1: Parâng Granites; 2: Metamorphic rocks; 3: Early Jurassic (limestone); 4: Late Jurassic (limestone); 5: Late Cretaceous (conglomerates, sandstones and clays); 6: Early Miocene (marly clays); 7: Middle Miocene (sands and clays); 8: Late Miocene (gravels and sands); 9: Caves; 10: Rivers. Inset: location of the Muierilor Cave within the Southern Carpathians (red arrow). (For interpretation of the references to colour in this figure legend, the reader is referred to the web version of this article.)

metamorphic pre-Alpine formations pierced by granitic bodies (Hann et al., 1986; Iancu and Seghedi 2017) that make up the main ridge of the Southern Carpathians. Sedimentary deposits are located along the mountain sides, outcropping as east-west oriented stripes of Upper Paleozoic and Mesozoic limestones and conglomerates and Cenozoic gravels, sands and clays (Figs. 1 and 2). During the uplift of the Carpathians, rivers flowing southward such as Olteț and Galbenul cut short but deep gorges into the limestone stripes and lead to the formation of extensive tiered cave systems.

The karst area of Polovragi – Cernădia is made up of Upper Jurassic-Lower Cretaceous (Aptian) limestones, also known as the Oslea – Polovragi Formation (Bandrabur and Bandrabur 2010). This formation consists of white-grey or white limestones with poorly developed exokarst, except for the Galbenul and Oltețului gorges. The limestones have a thickness of 150–250 m in the Galbenul Valley that gradually decrease to the northeast, and extends at surface over 0.8–2 km^2.

2.2. Cave morphology

Muierilor (45°11'31.78" N; 23°45'14.07" E) is a tiered karst system carved in the Upper Jurassic - Lower Cretaceous limestones, on the right side of the Galbenul Gorge (Fig. 2). The cave is accessed through two entrances (Northern and Southern, respectively) located at *c*. 645 m a.s.l. that give access to Level 2 (the show cave). Two upper levels (3 and 4) exist, although the latter is not physically connected to the main system. A lower Level 1 contains most of the fossil remains as a bone jumble embedded within sediments or lying on top of them. A so-called Level 0 is located only a couple of meters above the Galbenul River level and includes submerged passages that are only partially explored (Fig. 3).

The cave network broadly trends NNW-SSE, matching the main local fracture lines. It was created by dissolution along local fracture systems, simultaneously with the incision of Galbenul River (Diaconu and Medeșan, 1975). The cave functioned as a vertical succession of underground meanders of the surface river through lateral catchments of part of its waters (Ion and Lupu 1962). This pattern is currently encountered in Level 0, where subterranean water levels closely follow those of the surface river, as well as within the nearby Polovragi Cave (see Fig. 1). The cave system has a total length of more than 8000 m and is developed over an elevation range of ~80 m.

The major parts of the cave system include the Touristic Passage (Level 2) and the Scientific Reserve (Level 1), which have a total length of *c*. 5600 m and are connected by 10–15 m-deep shafts. Currently, all levels are hydrologically inactive except for Level 0 which is totally flooded during high water levels of the Galbenul River. The Touristic Passage follows a roughly N-S direction, parallel to the western side of the gorge, at some 50 m above the river. The passage is connected to the surface through three entrances and includes several large chambers (The Altar, The Turk, and The Guano chambers) connected through relatively narrow passages.

The Scientific Reserve (Level 1) includes the Bears, Hades, and Electricians passages and consists of broadly horizontal passages with several large chambers mainly oriented NNW-SSE and side-passages oriented NE-SW. The Bears Passage (*c*. 800 m) is accessed from the Touristic Passage via a series of short pits. More than 35 cave bear skulls and many other bone remains were found during the early exploration of this passage across a surface of only 50 m^2 (Fig. S1 A). The floor of this passage is covered by an abundant deposit of red clay with many speleothems such as stalagmites and flowstone grown on top or engulfed into it. The newly discovered Hades Passage (*c*. 900 m) is the most pristine section of the cave and hosts coarse alluvial sediments, many speleothems, fossil remains, including articulated skeletons (Fig. S1 B), coprolites and ichnofabrics. The Electricians Passage (*c*. 800 m) is the

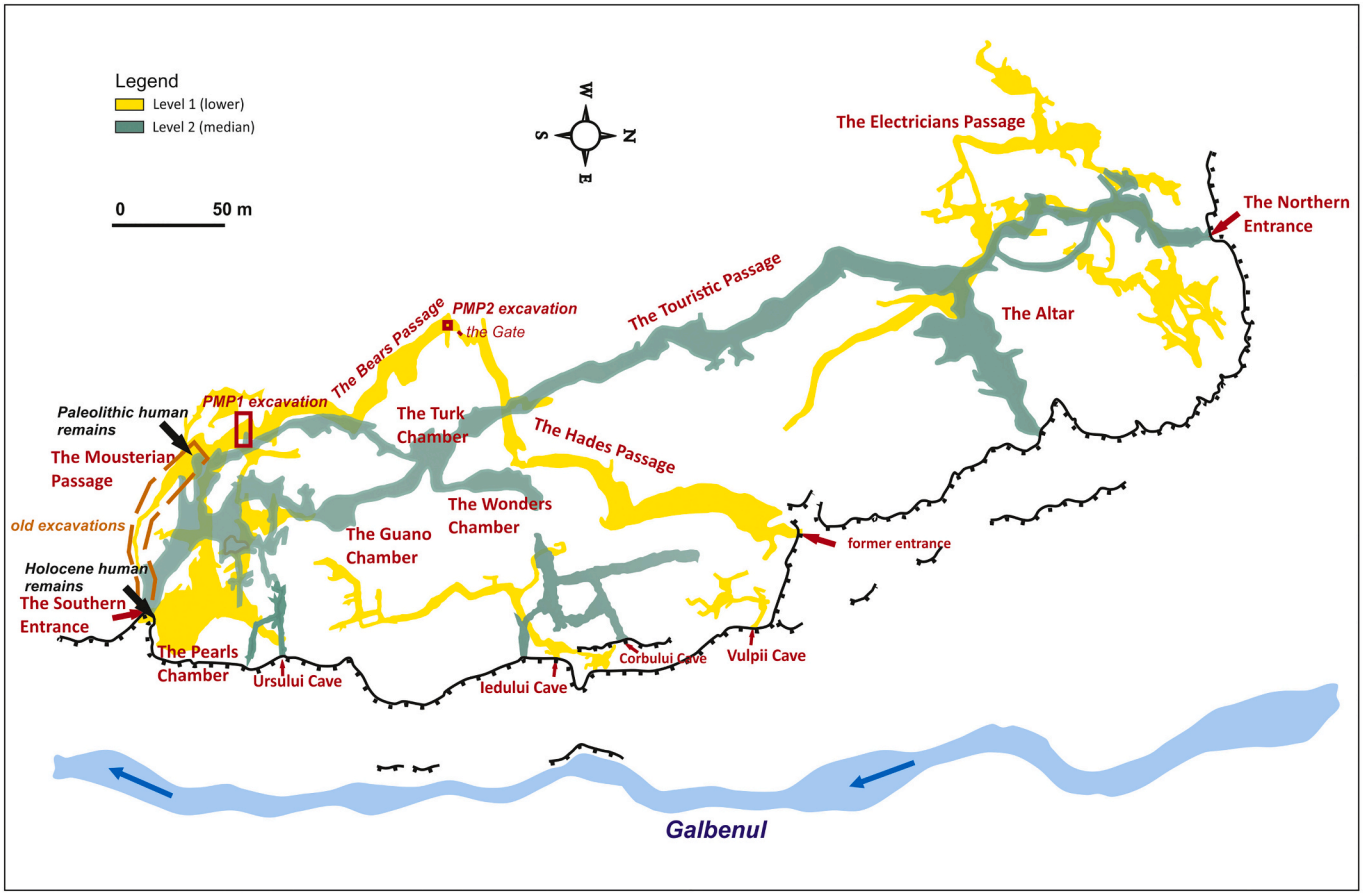

Fig. 2. Simplified map of Muierilor Cave system (surveyed by the "Hades" Caving Club and the "Emil Racoviță" Institute of Speleology).

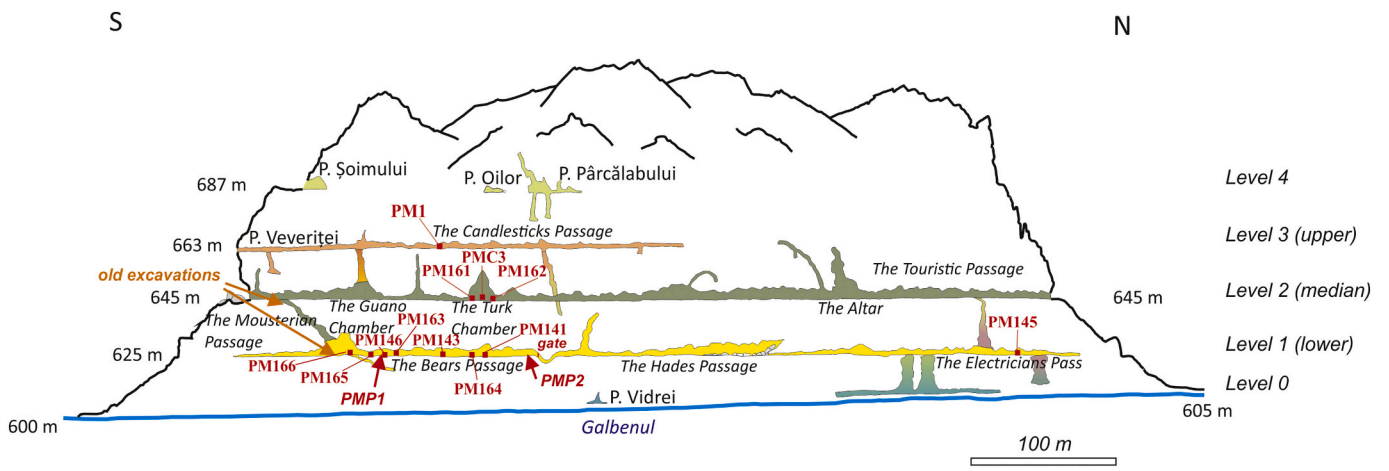

Fig. 3. Simplified section of Muierilor Cave system showing all five levels across the limestone massif, the positions of the U–Th dated speleothems (red rectangles), and the two excavations (PMP 1 and 2, red (arrows)) (modified after a sketch by the "Hades" Caving Club). (For interpretation of the references to colour in this figure legend, the reader is referred to the web version of this article.)

upstream segment of Level 1, and consists of a maze of generally small passages with massive deposits of loose sediments that include, in places, 15–20 m-deep suffosion shafts.

2.3. Cave deposits

Virtually, all cave passages contain alluvial sediments deposited by the Galbenul River and possibly some small tributaries. The primary source of sediments is considered to be the upper reaches of the valley, i.e. the alpine zone of the Parâng Mountains (*c.* 2500 m asl), an area that was glaciated during the Late Pleistocene (Gheorghiu et al. 2015). The sediments consist mainly of sands, silts and clays, with subordinate pebbles and cobbles. In some passages the sediment deposits are mixed with breakdown blocks; they often appear to be reworked and mixed with fossil remains and flowstone fragments.

Classical calcite speleothems, such as stalactite, stalagmites, and flowstone are present throughout the cave. They often overlie the sediments and fossil remains and are sometimes found as interbeds within the sediment layers. In the lower level, speleothems (small stalactites, flowstone) made of carbonate-hydroxylapatite (dahlite) [$Ca_5(PO_4)_3(OH)$] and brushite [$CaH(PO_4)\cdot 2H_2O$] were described by Diaconu et al. (2008); the source of phosphate is considered to be the guano and/or the fossil bones accumulated within the sediments.

Fossil remains are abundant in both main levels of the cave and sometimes they form bonebeds mixed with alluvial sediments. Muierilor hosts an impressive number of fossil remains mostly belonging to Late Pleistocene cave bears (*Ursus spelaeus* Rosenmüller, 1794), cave lions (*Panthera spelaea* Goldfuss, 1810), cave hyenas (*Crocuta crocuta spelaea* Goldfuss, 1823) and wolves (*Canis lupus* Linnaeus, 1758) as described within the previous excavations (Bombiță 1954; Nicolăescu-Plopșor 1957; Doboș et al. 2009; Doboș et al. 2010). MIS 3 herbivore and small mammals' remains were also found (most of them within the Touristic, Mousterian and Bears passages). Holocene human remains were found in the Southern entrance area, and Upper Paleolithic human remains were discovered much deeper in the cave, in the Mousterian Passage (Nicolăescu-Plopșor 1938; 1957; Păunescu 2001; Păunescu et al. 1982).

2.4. Studied profiles

Taking into account the general cave topography, the presence of a large number of fossil remains within the Bears Passage and further on along the Mousterian Passage, we carried out a new palaeontological excavation (PMP1) in the southern end of the Bears Passage (Fig. 2). Our working hypothesis was that the entrance path for the fossil remains was directed from north to south through the lower Level 1 of the cave system and that the remains accumulated at the southern end of the Bears Passage behind a natural obstacle such as a narrowing of the passage. The presence of an increasingly large number of cave bear skulls on the surface towards the southern end was an argument for this scenario. The surface faunal assemblage (including the ages of the human remains in the Mousterian Passage) suggested an MIS3 accumulation.

To test this hypothesis, we excavated the PMP1 trench which extends transversally across the Bears Passage's southern end for 9 m^2 and reaches depths of 60 to 240 cm. The trench was designed to intercept the entire width of the Bears Passage and to reveal the palaeohydrological features during the deposition of the fossil remains (Figs. 2 and 4).

A second excavation, PMP2, was done in the northern end of the Bears Passage, a few meters before its narrow connection with the Hades Passage (Figs. 2 and 3). PMP2 is a test pit of 1.5/1.5 m and with a depth of 4.8 m. The purpose of this excavation was to test for changes in sedimentology and taphonomy along the Bears Passage.

3. Investigation methods

3.1. Excavations

In both PMP1 and PMP2 excavations, 1 m^2 quadrants were established and bone samples were recorded, photographed and surveyed on the excavation grid and on a 10 × 10 cm sub-grid for each quadrant using the same excavation protocol in Constantin et al. (2014). To better understand the provenance of the fossil remains we carried out preliminary spatial orientation analysis on the long bones [$N = 105$: humeri ($N = 34$), ulnae ($N = 20$), tibiae (N = 20) and femora ($N = 31$)] extracted from the first two levels of the excavation (*c.* 20–25 cm below the "0" datum). The bone surveying was done using high-resolution pictures and by measuring the azimuth with a compass (ST = 5°), with the results being plotted as a rose-diagram.

3.2. Sediment analyses

To better understand the cave sediments dynamics, we surveyed on-site lithological logs, performed grain-size analyses of fine sediments, and measured the anisotropy of magnetic susceptibility (AMS) in both excavations. Grain size measurements were performed on a HORIBA Partica LA-950 V2 laser scattering particle size distribution analyzer following the same protocol used for other cave sediments (Constantin et al. 2014; Moldovan et al. 2016). In PMP2, the AMS was measured on

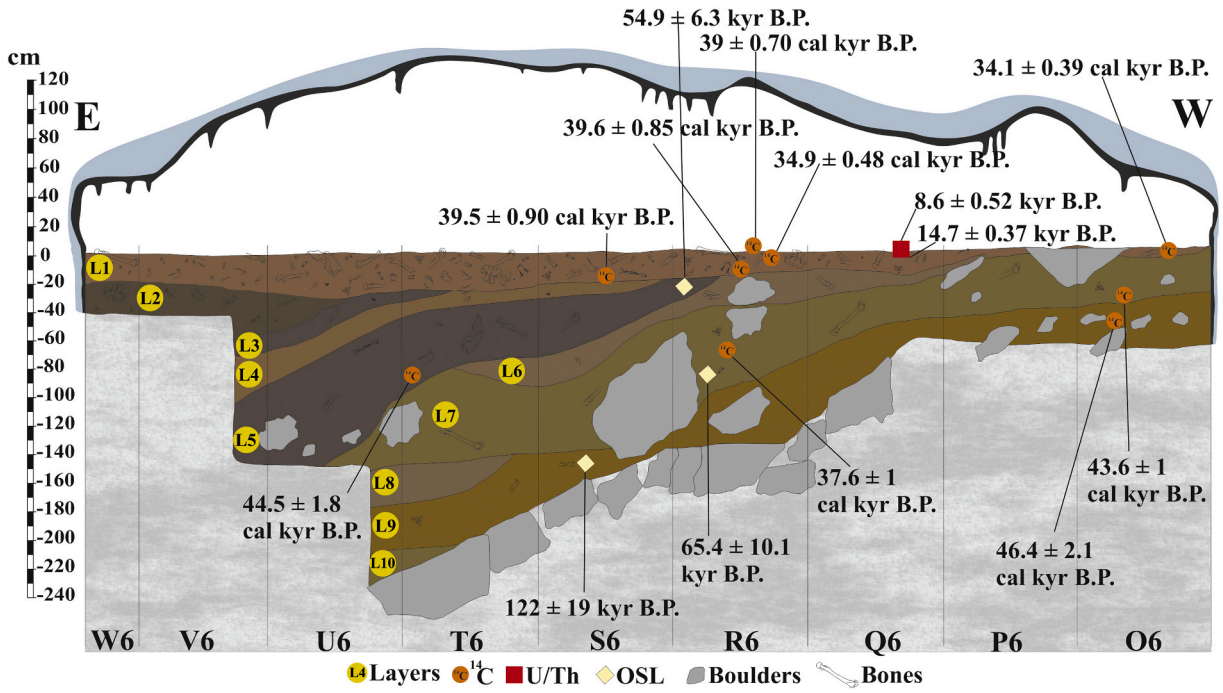

Fig. 4. Stratigraphic section of the PMP1 excavation trench of Bears Passage and dating results.

41 oriented samples (420 cm) whereas in PMP1 it was not possible to take a sufficient number of samples for this analysis because the profile is mainly made of coarse sediments, boulders and bones. Samples were collected in plastic cylinders (11cm^3) in-house designed to avoid rotation of sediments during the sampling and measurements. The AMS measurements were carried out using a 3D rotator coupled with the MFK1-A Kappabridge (AGICO). The AMS data were analyzed using Anisoft 5.1.01 (AGICO). Both grain-size and AMS measurements were done in the laboratories of the University of Bucharest.

3.3. Optically stimulated luminescence dating

Sediment samples for Optically Stimulated Luminescence (OSL) dating were collected by hammering 20 cm long plastic opaque tubes into the sediment sections, under no light conditions, both in the excavation trench (PMP1; 4 samples) and in the test pit (PMP2; 5 samples). The OSL dating was done at the Environmental Radioactivity and Nuclear Dating Centre (Babeș-Bolyai University) following the same protocol as in Constantin et al. (2014). Since the sediment-water content has strong effects on resulting age estimates (e.g. Zander and Hilgers 2013), we computed the age using both the "as found" water contents and by assuming a 30% water content. The later value is probably a better approximation of the moisture conditions in the cave sediments during the period of burial being close to the maximum values measured in our samples.

3.4. U–Th dating

Speleothem samples were collected from stratigraphically relevant positions from levels 1 through 3 of the cave system. A total of 12 speleothems were dated including 11 stalagmites and 1 flowstone core (Fig. 3). Stalagmite PM1 was collected from the Snails Passage in the upper Level 3 and dated (4 subsamples) by alpha spectrometry at the University of Bergen, Norway (Constantin, 2003) following the analytical procedures described in Constantin et al. (2007). The rest of 11 speleothems were dated at the Neptune Isotope Laboratory, Miami University, USA using a Thermo Fisher–Neptune Plus MC-ICP-MS. Calcite subsamples (100–200 mg) were hand-drilled along speleothem laminae in stratigraphically-relevant positions. Minimally, stalagmite bases were dated but often additional samples were dated from speleothem top layers, as well as across hiatuses. Chemical treatment, nuclides separation, measurement procedure, and propagation of random and systematic uncertainness are described in Pourmand et al. (2014). In total, 49 speleothem subsamples were dated, but in this study we only report the 16 ages of subsamples from stratigraphically-relevant positions.

3.5. AMS ^{14}C dating

Bone samples for radiocarbon dating were collected from Bears (surface and excavation) and Hades passages (surface and two samples from a test pit). The AMS ^{14}C dating (31 bone samples) was done commercially at the Poznan Radiocarbon Laboratory (Poland). Analytical procedures were the ones described by Longin (1971) with further modifications (e.g. Piotrowska and Goslar 2002). The bone treatment followed the method described by Brock et al. (2010), including the collagen extraction, purification (using Elkay 8 μm filters) and ultrafiltration (Vivaspin 15 MWCO 30 kd filters). The $^{14}C/^{12}C$ ratio in the C–Fe mixture was measured using the AMS spectrometer as described by Goslar et al. (2004). The calibration of AMS ^{14}C ages was performed using the program OxCal ver. 4.4.2 (Bronk Ramsey 2009, 2020) against the INTCAL13 radiocarbon calibration curve (Reimer et al. 2020).

4. Results

4.1. Stratigraphy and sedimentology

The PMP1 excavation trench reached a maximum depth of 260 cm in its central part. A total number of 10 sediment layers were identified (L1 through 10, see Fig. 4 and Fig. S1 C-E). The first 30 cm (L1) are rich in large mammal fossil remains and the sediment matrix consists of a mixture of red clay, silt, and large-sized allogenic clasts. The highest occurrence of the fossil remains was found in the median area of the trench (T6 and S6 squares). L1 and L2 are the richest bone layers excavated, including almost exclusively bones and very scarce, if any, sediment matrix (e.g., V6 and W6 quadrants). L6 corresponds to a 40 cm

sedimentation stage characterized by fluctuations in transport dynamics that generated successive channels filled by sediments and bones of L3, L4, and L5 layers. In L7, L8, L9 and L10, the density of the palaeontological material decreases and large-size breakdown blocks were found. Here sediments consist of a mix of large-size allogenic clasts and abundant large fossil remains, indicative for rapid reworking processes over relatively short-distances and with high transport energy. These are common features for all major sediment layers (L1, L5, L7, L9) from the excavation trench. The fossil accumulation is represented mostly by scattered skeletal fragments belonging to cave bears, cave lions, cave hyena, wolf and scarce elements of herbivores (red deer, ibex, and bison) and micromammals. The 5–20 cm-thick of red-clay deposited at the surface of the Bears Passage, north of PMP1 and engulfing scattered cave bear remains (skulls, long bones) and speleothems was denominated as L0 (or "Surface") since it is clearly younger than L1. This was considered as being deposited from a low-energy hydraulic event that deposited most of the sediments north of the excavation owing to cave floor topography.

The PMP2 test-pit (Fig. S1 F) shows a complex structure with levels of sands, silts and clays. Within the first three meters from the bottom, sediments are alternating sand and silt (Figs. 5 and S2). Higher amounts of clay appear towards the upper part, while in the topmost part alternating clay and sands suggest a higher energy current.

4.2. OSL dating results

Of nine collected sediment samples, seven were suitable for dating. The values for radionuclide concentrations, the total dose rates, the average De values and OSL ages are presented in Table 1. From the PMP1 profile, three samples were dated (Fig. 6). The sediment from the lower part of the PMP1 profile yielded the oldest OSL age of 122 ± 19 kyr B.P. The other two OSL ages from the upper layers are significantly younger: 65.4 ± 10.1 kyr B.P. and 54.9 ± 6.3 kyr B.P.

The base of the sediments in the PMP2 profile has an OSL age of 74.7 ± 12.3 kyr B.P., while the last 2 m of the section shows apparent younger OSL ages of around 58 kyr B.P. (Fig. 6). Nevertheless, when taking into account the analytical uncertainties, the four ages measured for the PMP2 profile appear to be statistically equal.

4.3. U-series dating results

The U/Th dated speleothems yielded ages ranging between 119 ± 5 kyr B.P. and 11.6 ± 1 kyr B.P. (Fig. 7 and Figs. S3-S4; Tables 2 and 3). All samples had relatively good U-contents, ranging between 0.2 and 0.9 ppm. Most of the samples showed low $^{230}Th/^{232}Th$ ratios indicating a certain detrital contamination and requiring age corrections. The **PM1** stalagmite is a candlestick stalagmite that grew over sediment in Veveriţei Cave (Level 3). The four ages measured along its growth axis show a constant growth across Marine Isotope Stages (MIS) 5e through 5c (*c*. 120 through *c*. 90 kyr B.P.). Within Level 1, the base of the massive **PM143** stalagmite, which grew on a rocky terrace, yielded an age of 82 ± 5 kyr B.P. but this can only be considered as a maximum age due to the high Th contamination.

Most of the samples showed ages between *c*. 15–8 kyr B.P. The U-series dating results of the 11 speleothem sample bases from four passages (Touristic, Bears, Hades and Electricians passages) are given in Table 3. The **PM161** and **PM162** were sampled from Level 2 (Wonders Chamber, Touristic Passage), both growing on top of a flowstone deposit and yielding base ages of 28 ± 0.2 kyr B.P. and 19 ± 0.2 kyr B.P., respectively. **PMC3** is a 30 cm-long flowstone core sampled from Level 2 (Turk Chamber) that yielded a top age of 10.3 ± 0.7 kyr B.P. and dates the flowstone layer that covers the chamber floor. **PM141** was sampled from Bears Passage, where it was engulfed in the topmost 2 cm of the surface clay layer (L0). Its basal age of 11.7 ± 1 kyr B.P. pre-dates the moment of clay deposition. **PM146** is a small (ca 6 cm) stalagmite that grew directly on top of the L1 of the PMP1 excavation. This is a stratigraphically significant sample because its base age of 14.7 ± 0.3 kyr B.P. postdates the deposition of the L1, while its top age of 8.6 ± 0.5 kyr B.P. postdates the sedimentation of the surface clay layer L0 in Bears Passage. The rest of the speleothem samples from Bears Passage yielded mostly Holocene ages for base subsamples, with the exception of **PM163** which grew in a recess of the passage and yielded a basal date of 31.2 ± 0.2 kyr B.P.

4.4. Radiocarbon dating results

From a total number of 31 dated samples, we marked as questionable ages the results that either show abnormally low %N (<0.5%) or collagen yields lower than 0.6% ($N = 16$). All radiocarbon data are falling within the MIS 3 (Table 4, Figs. 8 and S3). The age dating results from the Bears Passage, collected both from surface and the palaeontological excavation, range between *c*. 46–27 cal kyr B.P. (median values; N = 13). Radiocarbon results from the Hades Passage ($N = 4$) show a time range between *c*. 48–37 cal kyr B.P. (median), indicating rather older ages than the Bears Passage. All radiocarbon dated bone samples from the Hades Passage show a negative $\%C_{ncoll}$, ranging between −0.64% and − 0.04%. This depletion in non-collagen can be explained, most probably, by their location on the sediment surface which favored collagen loss (Doboş et al. 2010). The questionable ages from the Bears Passage range between 46.4 and 22.5 cal kyr B.P. and have low collagen yields (0.1–0.8%). Some cave bear samples with questionable ages, like Poz-87,737 (18.6 ± 0.18 kyr B.P.), have a computed C/N ratio (3.2) within the accepted range (2.9–3.6) allowing them to be cautiously taken into consideration. Nonetheless, the age of these samples is in agreement with the reliable radiocarbon and the OSL results, with all of them indicating a reversed chronology and reworking of the deposits.

5. Discussion

5.1. Fossil bone accumulation

The MIS 3–2 cave bear complex from Muierilor, can be classified in two categories of bone accumulations: (i) a primary thanatocoenosis (deposited *in situ*, with fully or partially articulated skeletons – typical to Hades and Electricians passages) and (ii) a secondary thanatocoenosis including a reworked bone deposit (=taphocoenosis – typical to Bears and Touristic passages) accumulated during significant hydraulic events (palaeofloods) followed by the deposition of more fragile bones (e.g. skulls) on the surface (=thanatocoenosis *per se*).

In Level 3, scattered fossil remains and palaeoichnofabrics, mostly weathered and poorly preserved, were identified on the palaeosurface and in side-passages. In Level 2, fossil remains were found mostly in secondary chambers and side-passages, as the touristic fitting of the main passage led to removal of most of the fossil remains. The largest bone accumulation in the studied karst system is undoubtedly the one located within the Bears Passage, where an extremely high density of fossil remains (sometimes up to 200 bones/m^2) was documented in the PMP1 excavation.

The PMP1 excavation (Figs. 4 and S1 C-E) yielded a large number of fragmented and broken fossil bone remains (*c*. 10,000 bones and bone fragments). Based on the spatial assessment of the long bones located within the first 50 cm of the palaeontological excavation (Fig. S5), the main orientations seem to be NNW-SSE and ENE-WSW, which are consistent with the generally inferred N-S paleo-flow direction but also suggest that the fossil remains were transported under a turbulent hydrodynamic regime. This is consistent with the grain-size analysis showing a coarser sediment matrix in the lower levels and a finer one towards the surface.

At the surface of the Bears Passage the density of fossil remains, including cave bear skulls (fig. S1 A) is high at the southern end and decreases to total absence towards the narrow squeeze leading to the

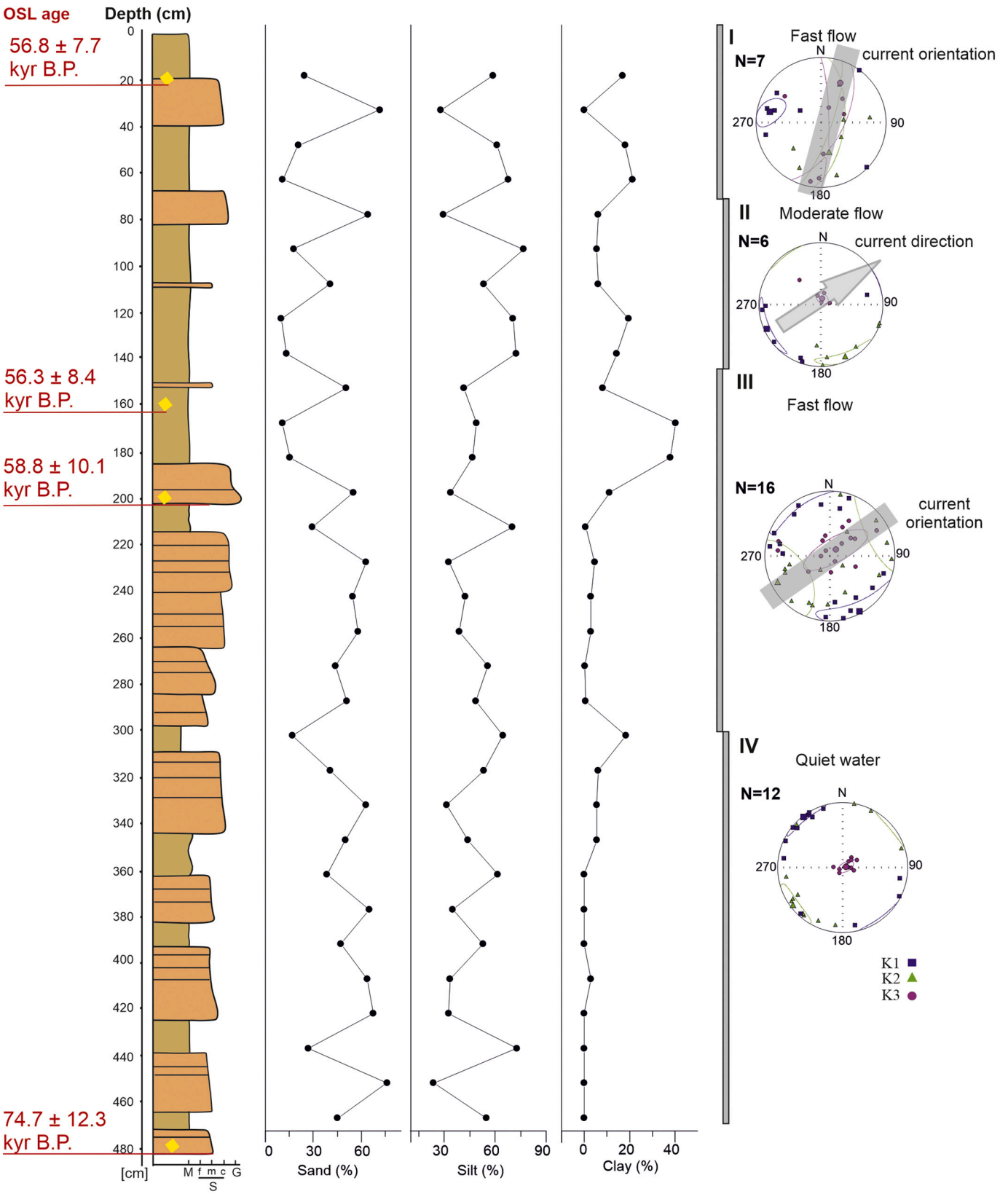

Fig. 5. PMP2 section (Bears Passage): the lithological log, grain size measurements, and lower hemisphere equal-area projections of principal directions of AMS ellipsoids for each sample: blue squares = maximum magnetic susceptibility K1; green triangles = intermediate magnetic susceptibility K2; purple circles = minimum magnetic susceptibility K3. Directions of mean AMS ellipsoid are represented with bigger symbols together with their 95% confidence ellipses. (For interpretation of the references to colour in this figure legend, the reader is referred to the web version of this article.)

Table 1
Summary of the luminescence and dosimetry data. Equivalent doses have been determined using 63–90 μm quartz. Ages in **bold** have been considered in this paper.

Sample code	Depth (cm)	Assuming water content as found (%)	ED (Gy)	U-Ra (Bq/kg)	Th (Bq/kg)	K (Bq/kg)	Total dose rate (Gy/kyr B.P.) assuming water content as found	Total dose rate (Gy/kyr B.P.) assuming 30% water content	Age (kyr B.P.) assuming water content as found	Age (kyr B.P.) assuming 30% water content
***Excavation* (PMP1)**										
OSL1	20	19.1%	114.0 ± 5.2 (n = 10)	53.8 ± 2.0	26.7 ± 1.1	363 ± 13	2.29 ± 0.05	2.08 ± 0.04	49.7 ± 4.6	**54.9 ± 6.3**
OSL2	90	8.6%	174.4 ± 19.4 (*n* = 8)	33.1 ± 1.4	31.3 ± 1.1	716 ± 17	3.28 ± 0.06	2.67 ± 0.05	53.2 ± 6.8	**65.4 ± 10.1**
OSL3	150	3.1%	155.8 ± 18.0 (n = 8)	26.5 ± 1.2	21.3 ± 0.6	227 ± 12	1.66 ± 0.04	1.28 ± 0.03	94 ± 12	**122 ± 19**
***Test pit* (PMP2)**										
OSL5	20	34.1%	190.7 ± 15.8 (n = 8)	36.9 ± 1.9	46.1 ± 0.6	901 ± 20	3.24 ± 0.05	3.36 ± 0.05	58.8 ± 8.4	**56.8 ± 7.7**
OSL6	160	30.9%	170.5 ± 17.9 (n = 8)	27.1 ± 2.1	46.7 ± 1.7	821 ± 20	3.01 ± 0.06	3.03 ± 0.06	56.7 ± 8.6	**56.3 ± 8.4**
OSL7	200	14.8%	177.7 ± 24.0 (n = 8)	29.0 ± 1.1	37.9 ± 1.1	855 ± 19	3.48 ± 0.06	3.02 ± 0.05	51.0 ± 7.8	**58.8 ± 10.1**
OSL9	480	4.1%	159.4 ± 20.2 (n = 8)	54.4 ± 2.2	14.0 ± 0.6	454 ± 13	2.75 ± 0.05	2.13 ± 0.04	57.9 ± 8.1	**74.7 ± 12.3**

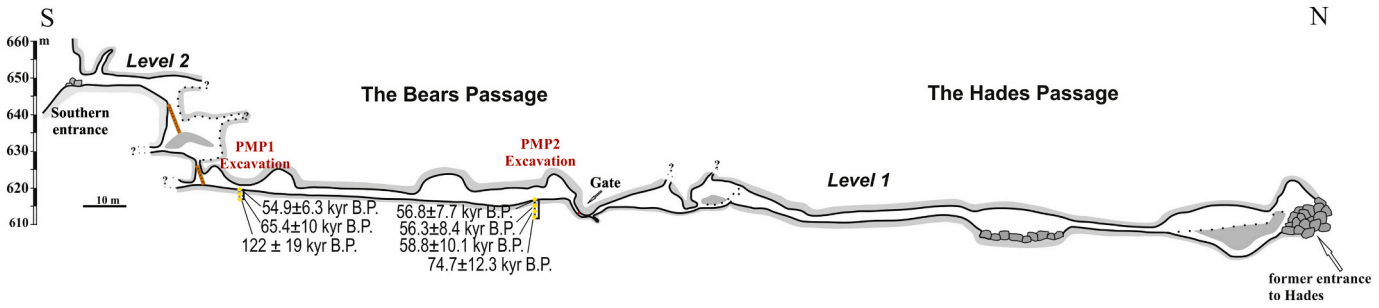

Fig. 6. Long profile through the Bears and Hades passages with the OSL results (yellow dots). (For interpretation of the references to colour in this figure legend, the reader is referred to the web version of this article.)

Hades Passage. Within the PMP2 test-pit no fossil remains were found. Here, the AMS data (Fig. 5) show that between 420 and 300 cm-depth the sedimentation took place at low hydraulic regime, from slackwaters (Ford and Williams 2013; Ballesteros et al. 2017). The next 150 cm are characterized by deposition under a higher current flow, while the next 50 cm show a distribution of both the minimum and maximum susceptibility axes which is compatible with deposition in moderate currents (i.e. no particle entrainment). We therefore assume that the flow direction was NE-SW with possible "apparent reversals", such as those due to vortex-type flows generated by cave walls topography.

The sediment plug formed between the Bears and Hades Passages appears to have been interrupted by the sediment transport from one passage to the other, with the Hades Passage preserving a couple of articulated skeletons as well as ichnofabrics and pristine calcite speleothems. The massive fossil deposit at the southern end of the Bears Passage was likely reworked from the northern sector of cave's Level 1, via the Hades Passage, until the last episode of low-energy flooding which deposited the surface red clay layer and cut the connection.

5.2. Geochronology

The radiocarbon ages of *Ursus* ex.gr. *spelaeus* samples indicate an almost continuous period of usage of Muierilor between (at least) 46 and 29 cal kyr B.P., suggesting synchronous co-usage of the entrances/passages by these large mammals and by the anatomically modern humans (Fu et al. 2016). However, when considering the distribution of the ages within the PMP1 deposit, it appears that no clear stratigraphy exists, even when discarding samples with low collagen yields. The PMP1 deposit rather appears as a strongly reworked mix of sediments that have been deposited into the cave starting at least ~120 kyr ago and showing an apparent peak between ~75–55 kyr ago and have been subsequently transported together with MIS3 bones or bone fragments by a strong NE-SW directed successions of floods.

The timing of these events is constrained by the youngest radiocarbon ages of fossil remains (*c.* 22.5 cal kyr B.P.) and the basal U–Th dating of the PM146 stalagmite that has "sealed" the Layer 1 at ~14.7 kyr B.P. If we discard all radiocarbon samples that have low collagen yields, the time range for sediments deposition extends between *c.* 34 and 14.7 kyr B.P., encompassing much of the MIS 3 and the MIS 2. The thin layer of fine clay (L0) that currently covers the floor of the Bears Passage was deposited at some time between *c.* 11.7 and 8.6 kyr B.P. as it engulfs the base of PM141 stalagmite but it is located below the top of the PM146. This last hydraulic event was a low-energy one, as indicated by its sedimentological features and the absence of bone remains.

Concerning the young radiometric ages of the cave bears (*c.* 27–22.5 cal kyr B.P.) we cannot rule out that cave bears might have survived during the Last Glacial Maximum (LGM) in the Southern Carpathians. Unpublished cave bear data from the Urşilor Cave, Western Carpathians (Robu, *pers. comm.*) indicate an even younger age for the same species (*c.* 20.5 cal kyr B.P.). In Poland, at Stajnia Cave, located in the Częstochowa Upland, at ~750 km NW from Muierilor, a cave bear sample yielded an age of *c.* 25.2 cal kyr B.P. (Baca et al. 2016), very close to the Muierilor youngest ages. We therefore hypothesize that the cave bear population in Muierilor area might have been one of the last documented to survive in Eurasia and that the foothills of the Southern Carpathians could have been a glacial refuge for this species during the LGM.

5.3. The general evolution of Muierilor system from MIS 5 through MIS 1

Based on the sedimentological research and dating of the various

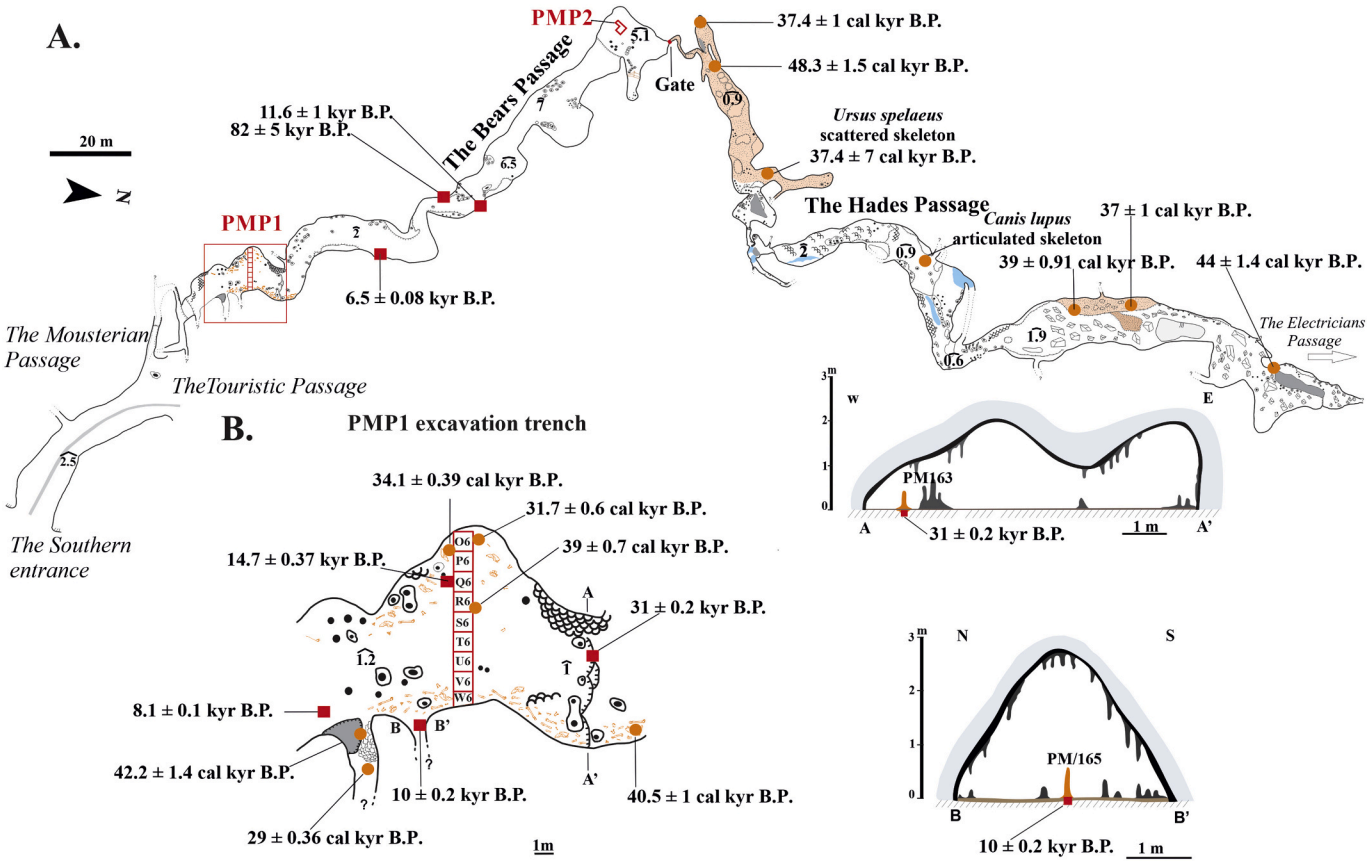

Fig. 7. A: Detail map of the Bears and Hades passages with the position of sedimentological sections and dated samples. B. Detail map of the Bears Passage around the PMP1 excavation trench with the position of dated samples and cross-sections showing the position of relevant speleothems. Legend: red squares = U-Th data; yellow diamonds = OSL data; orange circles = calibrated ^{14}C data. (For interpretation of the references to colour in this figure legend, the reader is referred to the web version of this article.)

Table 2
Summary of the U/Th by alpha spectrometry on stalagmite PM1 (Snails Passage). All ratios are activity ratios and all uncertainties are 1σ. Ages in **bold** are considered reliable and have been taken into account in this paper.

Sample name and position	U cont. (ppm)	$^{234}U/^{238}U$	$^{230}Th/^{234}U$	$^{230}Th/^{232}Th$	Age (kyr B.P.)	+err −err	Corr. age (kyr B.P.)	+err −err
PM1/1 0–2 cm	0.524 ± 0.010	1.437 ± 0.028	0.697 ± 0.017	57.2	**119.03**	**+4.95 −4.76**		
PM1/2 4–6 cm	0.252 ± 0.005	1.418 ± 0.028	0.692 ± 0.018	36.2	**117.89**	**+5.17 −4.96**	115.05	+5.26 −5.05
PM1/3 24.5–27 cm	0.446 ± 0.008	1.426 0.026	0.631 ± 0.014	37.2	**101.27**	**+3.63 −3.53**	98.72	+3.70 −3.60
PM1/4 top 61–63 cm	0.288 ± 0.012	1.313 ± 0.069	0.582 ±0.028	49	**90.55**	**+6.66 −6.31**	88.72	+6.76 −6.41

cave deposits in Muierilor, a broad scenario emerged, highlighting key-phases of the cave system evolution during the last 120 kyr B.P. (MIS 5–1) (Lisiecki and Raymo 2005) (Fig. 9):

5.3.1. MIS 5 (c. 130–71 kyr B.P)

MIS 5 is known worldwide for the alternation of climatic conditions, including climatic optimums such as the Eemian and colder and drier stadials (Rasmussen et al. 2014). At the end of the MIS 5e, stalagmite PM1 (*c.* 119 kyr B.P.) started to grow on sediments in Level 3, indicating that this level was already functioning as a hydrologically inactive passage and the climatic conditions were favorable for the development of a soil cover and cave calcite precipitation. On the other hand, the OSL3 sample (122 ± 19 kyr B.P.) suggests sediment input in Level 1 during the Eemian while the PM143 stalagmite, started to grow on a rock terrace of the same level at the beginning of MIS 5a (*c.* 82 kyr B.P.). This last age suggests that by MIS 5a the underground river had deepened sufficiently to allow for at most vadose flow and subaerial calcite precipitation in the upper levels of the system.

5.3.2. MIS 4 (c. 71–57 kyr B.P)

The only ages that correspond to MIS 4 are those of the OSL-dated clastic sediments from PMP1 and PMP2 (*c.* 74 through *c.*55 kyr B.P.) They suggest a relatively constant input of fine sediments (mostly sands and silts) in Level 1 passages. The MIS 4 period is generally known for the emergence of a cold continental climate with a lowering of both temperature and evaporation. Although no speleothem data exists for this time in Muierilor, speleothems are known to have grown during MIS 4, although at a reduced rate, in the nearby Cloşani Cave (Constantin and Lauritzen 1999; Constantin et al. 2006). With the current information we can only assume that Level 1 passages functioned under a vadose

Table 3
Summary of the U/Th dates by MC-ICP-MS. All ratios are activity ratios and all uncertainties are 2σ. Ages in **bold** are considered reliable and have been taken into account in this paper.

Sample no.	Distance from base (mm)	Sample mass (g)	238 U (ppb)	(95% CI) +/−	(230Th/ 238 U)	(95% CI) +/−	(230Th/ 232Th)	(95% CI) +/−	Age (kyr B.P.)	(95% CI) +/−	(234 U/ 238 U) initial (corrected)	(95% CI) +/−	Corr. Age (kyr B. P.)	(95% CI) +/−
The Touristic Passage														
PM161.1	3.5	0.109	325	0.2	0.258	0.001	39.123	0.388	29.26	0.16	1.103	0.003	**28.73**	0.2
PM162.1	10	0.126	324	0.2	0.204	0.001	19.279	0.262	20.6	0.11	1.191	0.003	**19.83**	0.22
PMC3.1	top 5 mm	0.126	251	0.17	0.099	0.001	107.719	16	10.4	0.072	1.092	0.003	**10.33**	0.07
The Bears Passage														
PM141.1	1	0.090	250	0.17	0.164	0.001	2.919	0.030	15.78	0.14	1.224	0.003	**11.69**	0.1
PM143.1	1	0.151	372	0.26	0.735	0.003	2.704	0.012	103.4	0.64	1.223	0.005	**82.12**	0.58
PM146.1	3	0.077	498	0.55	0.176	0.001	8.319	0.101	16.23	0.11	1.280	0.004	**14.78**	0.38
PM146.t	42	0.184	465	0.33	0.118	0.001	3.892	0.026	10.79	0.063	1.254	0.003	**8.66**	0.53
PM163.1	1	0.162	638	0.56	0.302	0.001	49.950	0.274	31.67	0.17	1.208	0.004	**31.23**	0.2
PM164.1	1	0.080	458	0.29	0.069	0.001	19.156	0.402	6.81	0.05	1.145	0.003	**6.54**	0.09
PM165.1	5	0.105	1000	0.57	0.124	0.001	11.197	0.088	10.94	0.056	1.302	0.003	**10.19**	0.19
PM166.1	1	0.122	848	0.54	0.093	0.000	15.015	0.081	8.58	0.036	1.228	0.003	**8.14**	0.11
The Electricians Passage														
PM145.1	1	0.112	207	0.17	0.263	0.001	2.897	0.018	16.41	0.084	1.897	0.006	**12.15**	0.10

hydraulic regime being periodically flooded at high levels of the Galbenul River.

5.3.3. MIS 3 (c. 57–29 kyr B.P)

The MIS 3 climate was characterized by short periods of abrupt warming and gradual periods of cooling of the climate (Rasmussen et al. 2014; Staubwasser et al. 2018). From a palaeoecological point of view, it was one of the most dynamic and rich periods of the cave evolution, as the MIS 3 large mammals and the first modern humans intensively used this karstic system as shelter. MIS 3 climate allowed for the thriving of Late Pleistocene fauna at Muierilor as well as in many other sites across Carpathians. The vast majority of the radiocarbon data of the fossil remains from Muierilor belong to this phase (between *c*. 46 and 30 kyr B.P; Table 4 and S1). The fossil association dating to this period shows a great diversity including cave bears, cave hyena, cave lion, wolf, herbivores, and small mammals. Among the MIS 3 cave bear sites from the Romanian Carpathians – like Cioclovina, Oase and Urșilor caves (Quilès et al. 2006; Constantin et al. 2014; Robu 2015, 2016), which include almost exclusively cave bears – Muierilor has the most diversified fauna.

The youngest OSL ages from PMP1 and PMP2 test pit have relatively high uncertainties and may be attributed to either the end of the MIS 4 or the beginning of the MIS 3, depending on timescale used. However, the sedimentological analyses suggest that they were deposited in the cave at roughly the same stage and from the same source. We consider it plausible that these sediments were first deposited in the cave by early floods of the Galbenul River somewhere at the level of a former entrance to the Hades Passage (see Figs. 6 and 7), and later reworked together with the MIS 3 bone remains towards the Bears Passage.

In many palaeontological cave sites of Romania, the rapid climatic oscillations typical to MIS 3 are indicated to be the cause of repeated flooding that led to fossil accumulations. However, in the case of Muierilor the radiocarbon chronology is reversed, with older fossil remains being found in the upper layers. This suggests that (i) the fossil remains were reworked and embedded within a matrix of older sediments; (ii) this event or series of events took place at some time after 27–22 kyr B.P. (i.e. the youngest ages of the fossil remains in PMP1). At the same time, some of the speleothems from levels 1 and 2 of the cave were growing during the MIS 3 (five out of 13 samples), indicating that the climate was mild enough to allow for soil cover development and speleothem formation.

5.3.4. MIS 2 (c. 29–14 kyr B.P)

The MIS 2 comprises both the LGM and the deglaciation that followed. During the LGM the population of many large mammal species generally show a marked decrease in number, such as around 22.5 cal kyr B.P. the last cave bear individual was documented for this site. The lack of speleothem formation during the LGM was documented as well for other Romanian karst systems (e.g. Constantin et al. 2007; Staubwasser et al. 2018) with calcite precipitation resuming in some places (including Muierilor) as early as 15–14 kyr B.P. Coupled with the geomorphological and sedimentological evidence (which indicate a massive post-LGM remobilization of both sediments and MIS 3–2 fossil remains), one can state that during the deglaciation phase, the general climate warming triggered the flooding events that have re-shaped and complicated the stratigraphy across the greatest karst systems of the Romanian Carpathians (e.g. Constantin et al. 2014). Muierilor is no exception.

At the bottom (*c*. 2.3 m) of the PMP1 palaeontological excavation, a *c*. 22.5 cal kyr B.P. cave bear bone was recorded (*terminus post-quem*), while on the top of this profile the stalagmite PM146 started to grow at *c*. 14.7 kyr B.P. (*terminus ante-quem*). Although it is difficult to constrain precisely the geomorphological events that remobilized the older infillings in the Bears Passage, the age of deposition of the sediment stack corresponds to warming recorded at the end of the Heinrich 1 (H1) event and probably during the transition to the Bølling-Allerød (BA) interstadial. The H1 event was documented in Europe from various archives (e.g. marine sediments), producing major hydro-geomorphological impacts on the landscape (e.g. Menot et al. 2006; Soulet et al. 2011; Sanchi et al. 2014; Gheorghiu et al. 2015).

In the Southern Carpathians, Reuther et al. (2007), based on ^{10}Be exposure ages, documented for the southern slope of the Retezat Mountains (~80 km west of Muierilor) a post-LGM deglaciation stage after *c*. 16.1 kyr B.P. Only 25 km NE of Muierilor, in the central-northern area of the Parâng Mountains, Gheorghiu et al. (2015) showed, also using exposure dating, that the deglaciation of Late Würmian glacial complexes in the area occurred between *c*. 14.2–10.2 kyr B.P. In the Muierilor area, on the southern slope of the same massif, our radiometric data suggest an earlier start of the deglaciation, possibly coincident with the one recorded for the southern slope of the Retezat Mountains. Notably, the 14.7 kyr B.P. age determined for the stalagmite PM146, that marks the deposition of topmost sediments coincides with the peak of the Bølling oscillation. The earlier deglaciation at Muierilor and its amplitude may be explained by its geographical position on the southern vs. northern slopes of Parâng, and at a lower elevation than the sites studied by Gheorghiu et al. (2015).

5.3.5. MIS 1 (< 14 kyr B.P.)

During the MIS 1, and especially during the Holocene, the deposition of speleothem in Romanian caves is known to be abundant and extensive, to the point that often the Holocene formations totally cover older

Table 4
Results of radiocarbon AMS dating of fossil remains from Muierilor Cave. The radiocarbon dates were calibrated using the IntCal20 calibration dataset (Reimer et al. 2020). Qa = Questionable age.

Field no.	Lab no.	Specimen	Location	Depth (cm)	Coll. Yield (%)	% Cb	% Nb	% Cncoll	^{14}C age	cal yr B.P. age (median)	Age range cal yr B. P. (2σ)	Comments
The Bears Passage												
PM/GU-0-001	Poz-46,549	*U. spelaeus* canine	Scientific Reserve	Surface	0.7	1.0	0.2	0.46	30,270 ± 270	**34,296**	34,767–33,847	
PM/GU-0-002	Poz-46,543	*P. spelaea* metapodial	Scientific Reserve	Surface	3.3	6.4	2.9	−1.43	47,000 ± 2000	–	–	Qa
PM/GU-0-003	Poz-46,547	*U. spelaeus* M_2	Scientific Reserve	Surface	1.0	3.8	1.4	0.02	35,900 ± 500	**40,543**	41,572–39,495	
PM/GU-0-006	Poz-77,724	*C. lupus* M_1	Scientific Reserve	Surface	0.8	9.0	2.9	1.17	25,010 ± 140	**29,047**	29,431–28,711	
PM/GU-0-007	Poz-77,725	*Capra ibex* metapodial	Scientific Reserve	Surface	1.2	10.0	2.9	2.17	37,930 ± 860	**42,225**	43,698–40,870	
PM/O6–0-89	Poz-77,727	*U. spelaeus* mandible	Excavation	Surface	0.4	3.8	1.0	1.10	27,980 ± 210	**31,760**	32,500–31,295	
PM/O6–0-71	Poz-77,730	*U. spelaeus* I^3	Excavation	Surface	3.5	10.5	3.7	0.51	30,100 ± 210	**34,153**	34,572–33,793	
PM/R6–0-60	Poz-77,733	*U. spelaeus* mandible	Excavation	Surface	0.9	4.8	0.9	2.37	34,500 ± 330	**39,031**	39,806–38,396	
PM/R6-I-113	Poz-77,728	*U. spelaeus* mandible	Excavation	−10	1.2	5.5	1.6	1.18	31,090 ± 230	**34,990**	35,525–34,560	
PM/ U6-I-7	Poz-77,738	*U. spelaeus* canine	Excavation	−10	0.2	3.4	0.8	1.24	29,660 ± 310	**33,819**	34,414–33,205	Qa
PM/U6-II-25	Poz-77,754	*U. spelaeus* mandible	Excavation	−20	0.2	3.6	0.7	1.71	27,290 ± 240	**31,208**	31,535–30,899	Qa
PM/R6-II-14	Poz-77,739	*U. spelaeus* mandible	Excavation	−20	2.3	7.7	2.3	1.49	35,120 ± 360	**39,679**	40,530–38,820	
PM/O6-III-32	Poz-77,734	*U. spelaeus* canine	Excavation	−30	0.5	4.2	1.1	1.23	33,730 ± 310	**38,141**	38,855–37,056	Qa
PM/S6-III-10	Poz-87,733	*Bos* sp. metapodial	Excavation	−30	1.6	6.6	1.8	1.74	35,000 ± 400	**39,549**	40,474–38,667	
PM/U6-III-39	Poz-77,737	*U. spelaeus* mandible	Excavation	−30	0.2	2.9	0.7	1.01	28,420 ± 250	**32,354**	33,132–31,571	Qa
PM/O6-III-IV	Poz-77,732	*U. spelaeus* canine	Excavation	−35	1.2	5.1	1.9	−0.03	39,900 ± 600	**43,617**	44,705–42,689	Qa
PM/U6-III-IV	Poz-77,735	*U. spelaeus* mandible	Excavation	−35	0.4	2.6	0.5	1.25	33,960 ± 300	**38,455**	39,202–37,518	Qa
PM/O6-IV-V	Poz-77,729	*U. spelaeus* canine	Excavation	−45	1.25	7.6	4.0	−3.20	43,000 ± 1000	**46,443**	48,829–44,655	Qa
PM/P6-IV-V	Poz-77,731	*U. spelaeus* ulna frg.	Excavation	−45	0.1	4.1	0.9	1.67	21,320 ± 250	**25,633**	26,077–25,121	Qa
PM/U6-V-VI	Poz-87,734	*U. spelaeus* mandible	Excavation	−55	0.2	6.2	1.8	1.34	32,100 ± 300	**35,998**	36,671–35,300	Qa
PM/R6-VII-VIII	Poz-87,718	*U. spelaeus* metapodial	Excavation	−75	0.8	3.0	0.7	1.11	33,400 ± 400	**37,670**	38,635–36,535	
PM/T6-VIII-IX	Poz-87,735	*U. spelaeus* metapodial	Excavation	−85	1.6	8.0	6.0	−8.20	41,000 ± 1000	**44,594**	46,529–42,914	Qa
PM/T6-X-XI	Poz-87,719	*Bos* sp. tibia	Excavation	−115	0.6	3.4	0.5	2.05	22,850 ± 130	**27,214**	27,495–26,837	Qa
PM/T6-XIII-XIV	Poz-87,736	*U. spelaeus* M_1	Excavation	−135	0.2	3.6	0.7	1.71	22,200 ± 240	**26,465**	27,090–25,978	Qa
PM/T6-XVII-XVIII	Poz-87,737	*U. spelaeus* M_1	Excavation	−175	0.1	1.9	0.7	0.01	18,640 ± 180	**22,522**	22,974–22,090	Qa
PM/T6-XX	Poz-87,716	*U. spelaeus* canine	Excavation	−200	0.1	6.2	2.1	0.53	28,550 ± 380	**32,547**	33,529–31,554	Qa
The Hades Passage												
PM/GN-0-001	Poz-46,546	*U. spelaues* I_3	Scientific Reserve	Surface	0.7	2.8	1.2	−0.44	33,200 ± 370	**37,427**	38,427–36,425	
PM/GN-0-003	Poz-46,540	*C. lupus* canine	Scientific Reserve	Surface	1.0	5.3	2.2	−0.64	32,900 ± 360	**37,040**	38,213–36,171	
PM/GN-0-004	Poz-46,544	*U. spelaues* phalange	Scientific Reserve	Surface	0.4	2.1	0.9	−0.33	34,520 ± 420	**39,074**	40,086–38,261	Qa
PM/GN-X-005	Poz-46,545	*U. spelaues* M_1	Scientific Reserve	~ −30	0.7	3.2	1.2	−0.04	45,300 ± 1500	**48,360**	–	
PM/GN-0-006	Poz-46,542	*C. lupus* P_3	Scientific Reserve	Surface	1.0	3.6	1.5	−0.45	40,300 ± 900	**44,002**	45,611–42,633	

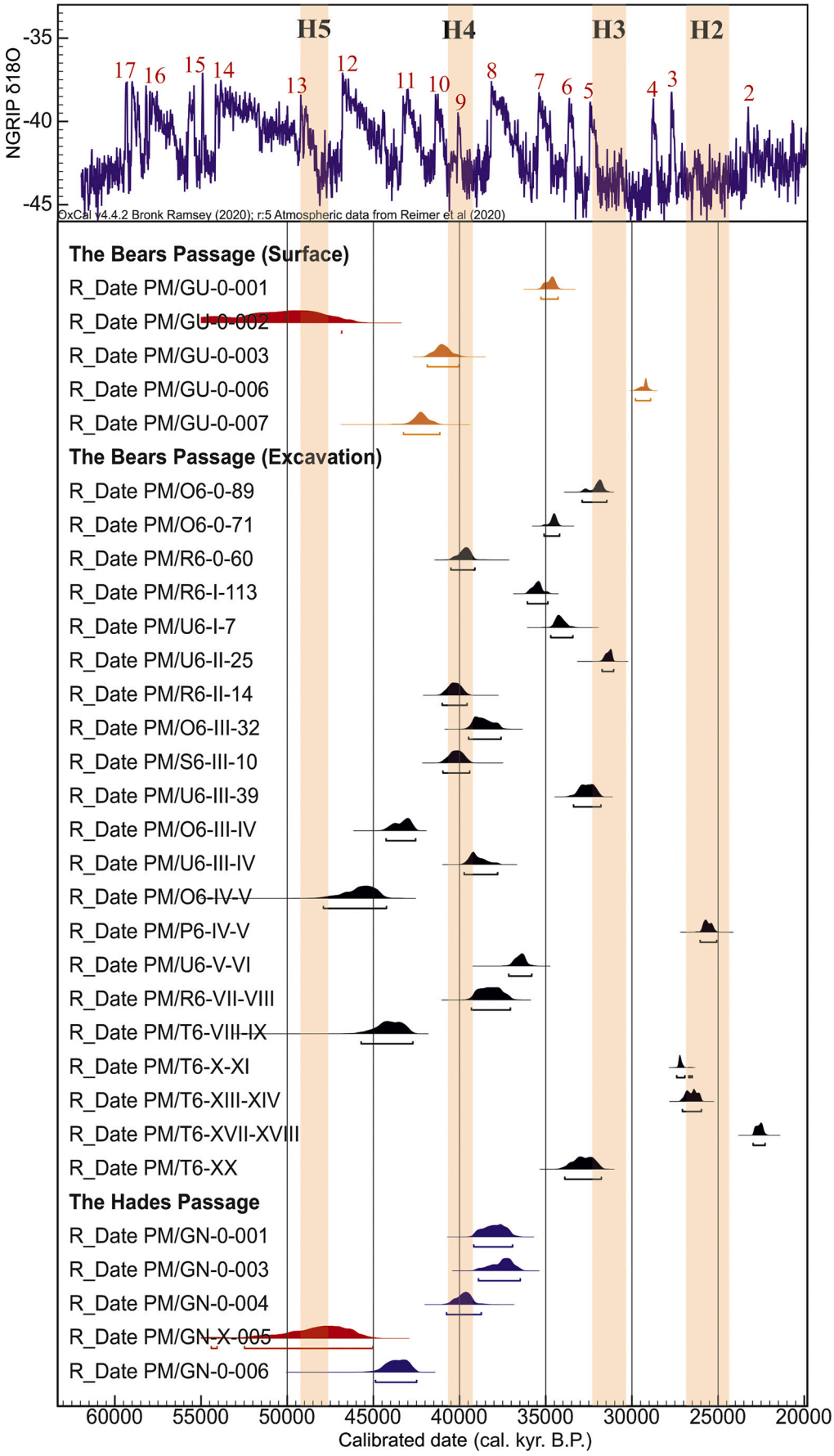

Fig. 8. Radiocarbon ages of the fossil remains from Muierilor Cave calibrated using OxCal ver. 4.4.2 (Ramsey, 2020) against the INTCAL13 radiocarbon calibration curve (Reimer et al. 2020). The NGRIP curve is shown for reference with the Heinrich (H) events marked. Note that samples in the PMP1 excavation are arranged stratigraphically in the figure (i.e. top levels first) and that the youngest ages appear at the bottom showing a reversed stratigraphy and sediments reworking. See Figs. 4 and 6, and Table 4 for samples descriptions and positioning.

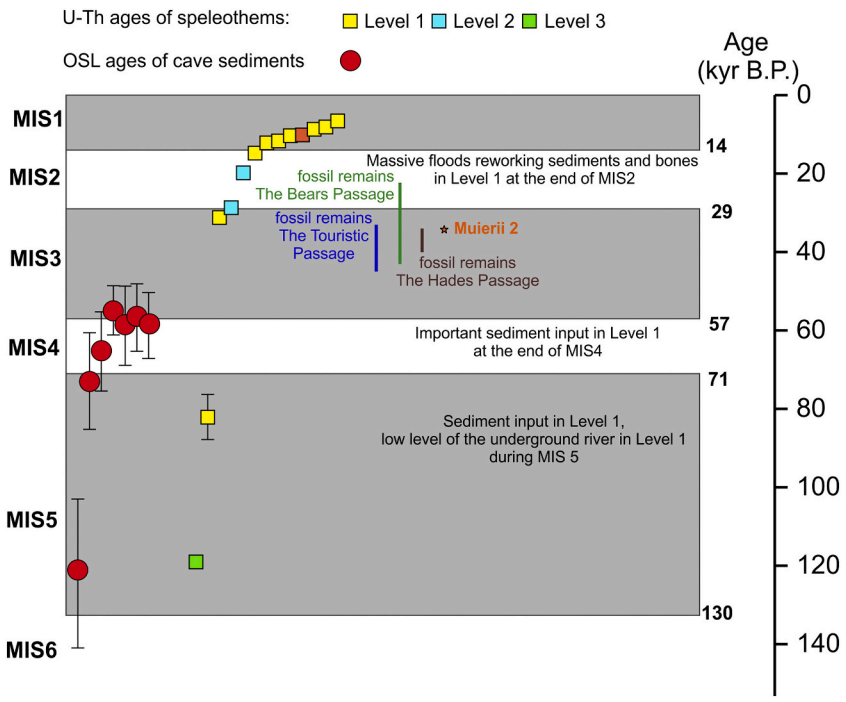

Fig. 9. Evolution model based on the radiocarbon, U–Th, and OSL samples during the MIS 5 through MIS 1.

speleothems or other deposits. This situation was documented for numerous Romanian caves (Onac et al. 2002; Constantin, 2003; Constantin et al., 2006; 2007; 2013; Drăguşin et al. 2014). Nine stalagmites from Muierilor provided base ages <14 kyr B.P., indicating fast calcite deposition and optimal climate conditions. In the Bears Passage, the L0 level of red clay appears to have been deposited from low-energy, stagnant waters, at some time between ~11.7 kyr B.P., (the end of the Younger Dryas), when the PM141 stalagmite started to grow and ~ 8.6 kyr B.P. (top layer of PM146). No further animal record or significant flooding was documented since, which may hint towards a significant incision of the Galbenul during the deglaciation, the end of usage of Level 1 passages as overflows, and possibly the clogging of some former entrances by collapses and/or flowstone deposition.

6. Conclusions

The sedimentological and geochronological work at Muierilor showed that the evolution of the cave system during the last 120 kyr was less influenced by discrete climatic pulses than previously thought. The combined OSL, U/Th, AMS ^{14}C and sedimentology results, together with taphonomical analysis of the Pleistocene mammals accumulation indicate that:

(1) Most cave levels were already formed at ~120 kyr ago with the uppermost level being hydrologically inactive during the MIS 5. During the same time and subsequently (at least MIS 4), the lower levels functioned periodically as vadose cave passages where sediments from the Galbenul River were deposited.
(2) A variety of animal species either inhabited the cave or used it as a shelter or depot (e.g. scavengers) with other remains being possibly transported in the underground by periodic flooding. Most of these remains were dated to MIS 3, which seems to have been a particularly favorable period for the thriving of many species.
(3) The young radiocarbon dates of some cave bears (~29–22.5 kyr B.P.) suggests that the lowlands of the Southern Carpathians may have been one of the last glacial refuges for this species during the LGM, although the data need further confirmation.
(4) Given the reverse chronology of the excavated MIS 3 fossil remains, these were clearly reworked during a post-MIS 3 stage. The U–Th dating of speleothems from stratigraphically-relevant positions suggests that the massive deposits of sediments and fossil remains were transported at some time shortly before ~14.7 ka, most probably during or at the end of the transition between the H1 event and the BA warming.
(5) The timing of the last deglaciation was tentatively established to be older than 14.7 ka, i.e. older than previously reported for the north of the same massif but plausible considering the geographical position on a southern slope and the low elevation of the cave.

This study shows that although a fossil assemblage may be properly assigned a certain age interval, the rather complicated functioning of a cave system may obscure the actual moment of its deposition. It also provides further proof that how speleothem U–Th dating may be key to constraining such events and complement investigation methods to decipher the evolution of cave systems.

Supplementary data to this article can be found online at https://doi.org/10.1016/j.palaeo.2020.110084.

Declaration of Competing Interest

None.

Acknowledgements

This research involved systematic excavation and research over the last seven years and therefore benefited from several sources of funding. It was initially supported through a National Geographic Grant (#964115) and further on through grants PCE 197/2016 (CARPATHEMS), and EEA 126/2018 (KARSTHIVES2), all to S. Constantin and RU-TE 2301/2014 (PALEOCLIM) to A. Petculescu. The support through grant PN-III-P4-ID-PCCF-2016-0016 (DARKFOOD, to O.T. Moldovan) is also acknowledged. We are grateful to Stelian Grigore, Cristinel Fofirică, Arthur Dăscălescu, Marius Iliescu ("Hades" Caving Club, Romania), the discoverers of the Hades Passage, for providing the base map of the cave

and for insightful discussions. We are also grateful to our colleagues Oana Moldovan, Virgil Drăguşin, Ştefan Baba, Sabrina C. Curran and to many other people who helped accomplishing this work: Costi Ispas, Gabriel Dan Chiriac, Marius Ciocănău, Laura Tîrlă, Simona Grădinaru. The authorities of Baia de Fier and the "White Wolf "Mountain Club are acknowledged for providing logistic support. Constructive criticism of Daniel Ballesteros and an anonymous reviewer helped us to improve the paper and are gratefully acknowledged. SC and AP designed research and secured funding. ICM, MR, AP, MK, LF, RA, VAC performed research, LF, RDR, and CGP have done the sedimentological study. SC, AliP, and AS have done the U-series dating, VT, MK, and ATG carried out the OSL dating. ICM, MR, and SC wrote the paper. All coauthors contributed to improve the manuscript.

References

Nicolăescu-Plopşor, C., 1938. Le paléolitique en Roumanie. Dacia 5–6, 1936–1953.

Constantin, S., 2003. Evoluţii paleoclimatice în Cuaternar pe baza speleotemelor din carstul Munţilor Banatului şi Mehedinţi. PhD Thesis. University of Bucharest, 324 p.

Álvarez-Lao, D.J., Ruiz-Zapata, M.B., Gil-García, M.J., Ballesteros, D., Jiménez-Sánchez, M., 2015. Palaeoenvironmental research at Rexidora Cave: New evidence of cold and dry conditions in NW Iberia during MIS 3. Quat. Int. 379, 35–46. https://doi.org/10.1016/j.quaint.2015.04.062.

Arriolabengoa, M., Iriarte, E., Aranburu, A., Yusta, I., Arnold, L.J., Demuro, M., Arrizabalaga, A., 2018. Reconstructing the sedimentary history of Lezetxiki II cave (Basque Country, northern Iberian Peninsula) using micromorphological analysis. Sediment. Geol. 372, 96–111. https://doi.org/10.1016/j.sedgeo.2018.05.006.

Baca, M., Popović, D., Stefaniak, K., Marciszak, A., Urbanowski, M., Nadachowski, A., Mackiewicz, P., 2016. Retreat and extinction of the late Pleistocene cave bear (Ursus spelaeus sensu lato). The Science of Nature 103, 92. https://doi.org/10.1007/s00114-016-1414-8.

Ballesteros, D., Jiménez-Sánchez, M., Giralt, S., DeFelipe, I., García-Sansegundo, J., 2017. Glacial origin for cave rhythmite during MIS 5d-c in a glaciokarstlandscape, Picos de Europa (Spain). Geomorphology 286, 68–77. https://doi.org/10.1016/j.geomorph.2017.03.014.

Ballesteros, D., Giralt, S., García-Sansegundo, J., Jiménez-Sánchez, M., 2019. Quaternary regional evolution based on karst cave geomorphology in Picos de Europa (Atlantic margin of the Iberian Peninsula). Geomorphology 336, 133–151. https://doi.org/10.1016/j.geomorph.2019.04.002.

Bandrabur, G., Bandrabur, R., 2010. Parâng and Capaţânii Mountains. In: Oraşeanu, I., Iurkiewicz, A. (Eds.), Karst Hydrogeology of Romania. Ed. Belvedere, Oradea, pp. 69–75.

Bombiţă, G., 1954. Mamiferele din glaciarul peşterilor de la Baia de Fier. Rezultate paleontologice ale săpăturilor din anul 1951. Bul. Ştiinţific, Secţiunea Ştiinţe Biol. Agron. Geol. şi Geogr. 6, 253–299.

Bradley, R.S., 2015. Paleoclimatology: Reconstructing Climates of the Quaternary: Third Edition. Elsevier.

Brock, F., Higham, T., Ditchfield, P., Ramsey, C.B., 2010. Current Pretreatment Methods for AMS Radiocarbon Dating at the Oxford Radiocarbon Accelerator Unit (Orau). Radiocarbon 52, 103–112. https://doi.org/10.1017/S0033822200045069.

Bronk Ramsey, C., 2009. Bayesian Analysis of Radiocarbon Dates. Radiocarbon 51 (1), 337–360. https://doi.org/10.1017/S0033822200033865.

Bronk Ramsey, C., 2020. OxCal online. https://c14.arch.ox.ac.uk/oxcal.html. Last accessed September 7, 2020.

Constantin, S., Lauritzen, S.-E., 1999. Speleothem datings in SW Romania. Part 1: evidence for a continuous speleothem growth in Pestera Closani during Oxygen Isotope stages 5-3 and its paleoclimatic significance. Theoretical and Applied Karstology 11-12, 35–46.

Constantin, S., Lauritzen, S.E., Lundberg, J., 2006. New data on the chronology of the Second Termination based on the isotopic study of a stalagmite from Closani Cave (South Carpathians, Romania). Archives of Climate Change in Karst, 10. Karst Waters Institute Special Publication, pp. 98–100.

Constantin, S., Bojar, A.-V., Lauritzen, S.-E., Lundberg, J., 2007. Holocene and late Pleistocene climate in the sub-Mediterranean continental environment: a speleothem record from Poleva Cave (Southern Carpathians, Romania). Palaeogeogr. Palaeoclimatol. Palaeoecol. 243, 322–338. https://doi.org/10.1016/j.palaeo.2006.08.001.

Constantin, S., Munteanu, C.-M., Milota, Ş., Sarcină, L., Gherase, M., Rodrigo, R., Zilhão, J., 2013. The Ponor-Plopa Cave System: Description, Sediments, and Genesis, in: Life and Death at the Peştera cu Oase: A Setting for Modern Human Emergence in Europe. Oxford University Press.

Constantin, S., Robu, M., Munteanu, C.M., Petculescu, A., Vlaicu, M., Mirea, I., Kenesz, M., Drăguşin, V., Hoffmann, D., Anechitei, V., Timar-Gabor, A., Roban, R.D., Panaiotu, C.G., 2014. Reconstructing the evolution of cave systems as a key to understanding the taphonomy of fossil accumulations: the case of Urşilor Cave (Western Carpathians, Romania). Quat. Int. 339–340, 25–40. https://doi.org/10.1016/j.quaint.2013.10.012.

Diaconu, G., Dumitraş, D., Marincea, Ştefan, 2008. Mineralogical analyses in peştera Polovragi (Oltetului gorges) and peştera Muierilor (Galbenului Gorges), Gorj County. Trav. L'Institut Speol. "Emile Racovitza" XLVII, pp. 89–105.

Diaconu, G., Medeşan, A., 1975. Spéléothèmes de dahllite dans la grotte "Pestera Muierii", Baia de Fier-Roumanie. Trav. L'Institut Speol. "Emile Racovitza", 14, pp. 149–156.

Doboş, A., Soficaru, A., Popescu, A., Trinkaus, E., 2009. Radiocarbon Dating and Faunal Stable Isotopes for the Galeria Principală, Peştera Muierii, Baia de Fier, Gorj County, Romania. Materiale şi cercetări arheologice, V 15–20. https://doi.org/10.3406/mcarh.2009.1066.

Doboş, A., Soficaru, A., Trinkaus, E., 2010. The Prehistory and Paleontology of the Peştera Muierii, Romania. ERAUL, Liege.

Drăguşin, V., Staubwasser, M., Hoffmann, D.L., Ersek, V., Onac, B.P., Veres, D., 2014. Constraining Holocene hydrological changes in the Carpathian-Balkan region using speleothem $\delta^{18}O$ and pollen-based temperature reconstructions. Clim. Past 10, 1363–1380. https://doi.org/10.5194/cp-10-1363-2014.

Dumitrescu, M., Tanasachi, J., Orghidan, T., 1963. Răspândirea chiropterelor în R.P.R. Trav. L'Institut Speol. "Emile Racovitza", 1–2, pp. 509–576.

Fairchild, I.J., Baker, A., 2012. Speleothem Science, Blackwell Quaternary Geoscience Series. John Wiley & Sons, Ltd, Chichester, UK. https://doi.org/10.1002/9781444361094.

Fairchild, I.J., Smith, C.L., Baker, A., Fuller, L., Spötl, C., Mattey, D., McDermott, F., 2006. Modification and preservation of environmental signals in speleothems. Earth-Science Rev. 75, 105–153. https://doi.org/10.1016/j.earscirev.2005.08.003.

Ford, D., Williams, P., 2013. Karst Hydrogeology and Geomorphology. https://doi.org/10.1002/9781118684986.

Fu, Q., Hajdanjak, M., Moldovan, O.T., Constantin, S., Mallik, S., Skoglud, P., Patterson, N., Rohland, N., Lazaridis, I., Nickel, B., Viola, B., Prufer, K., Meyer, M., Kelso, J., Reich, D., Paabo, S., 2015. An early modern human from Romania with a recent Neanderthal ancestor. Nature 524, 216–219, 13 Aug 2015. https://doi.org/10.1038/nature14558.

Fu, Q., Posth, C., Hajdinjak, M., Petr, M., Mallick, S., Fernandes, D., Furtwängler, A., Haak, W., Meyer, M., Mittnik, A., Nickel, N., Peltzer, A., Rohland, N., Slon, V., Talamo, S., Lazaridis, I., Lipson, M., Mathieson, I., Schiffels, S., Skoglund, P., Derevianko, A.P., Drozdov, N., Slavinsky, V., Tsybankov, A., Grifoni Cremonesi, R., Mallegni, F., Gély, B., Vacca, E., González Morales, M.R., Straus, L.G., Neugebauer-Maresch, C. Teschler-Nicola, M., Constantin, S., Moldovan, O.T., Benazzi, S., Peresani, M., Coppola, D., Lari, M., Ricci, S., Ronchitelli, A., Valentin, F., Thevenet, C., Wehrberger, K., Grigorescu, D., Rougier, H., Crevecoeur, I., Flas, D., Semal, P., Mannino, M.A., Cupillard, C., Bocherens, H., Conard, N.J., Harvati, K., Moiseyev, V., Drucker, D.G., Svoboda, J., Richards, M.P., Caramelli, D., Pinhasi, R., Kelso, J., Patterson, N., Krause, J., Pääbo,S., Reich, D., 2016. The genetic history of Ice Age Europe. Nature, 534:200–205, doi:https://doi.org/10.1038/nature17993.

Gheorghiu, D.M., Hosu, M., Corpade, C., Xu, S., 2015. Deglaciation constraints in the Parâng Mountains, Southern Romania, using surface exposure dating. Quat. Int. 388, 156–167. https://doi.org/10.1016/j.quaint.2015.04.059.

Goslar, T., Czernik, J., Goslar, E., 2004. Low-energy 14C AMS in Poznań Radiocarbon Laboratory. Poland. Nucl. Instruments Methods Phys. Res. Sect. B Beam Interact. with Mater. Atoms 223–224, 5–11. https://doi.org/10.1016/j.nimb.2004.04.005.

Hann, H., Berza, T., Pop, G., Marinescu, F., Ricman, C., Pană, D., Săbău, G., Bindea, G., Tatu, M., 1986. Harta geologică a României scara 1:50.000, foaia Polovragi. Institutul Geologic al României. Bucureşti.

Hatvani, I.G., Kern, Z., Leél-Össy, S., Demény, A., 2018. Speleothem stable isotope records for east-Central Europe: Resampling sedimentary proxy records to obtain evenly spaced time series with spectral guidance. Earth Syst. Sci. Data 10, 139–149. https://doi.org/10.5194/essd-10-139-2018.

Häuselmann, A.D., Häuselmann, P., Onac, B.P., 2010. Speleogenesis and deposition of sediments in Cioclovina Uscată Cave, Sureanu Mountains. Romania. Environ. Earth Sci. 61, 1561–1571. https://doi.org/10.1007/s12665-010-0470-1.

Iancu, V., Seghedi, A., 2017. The south carpathians: Tectono-metamorphic units related to variscan and pan-african inheritance. Geo-Eco-Marina 2017, 245–262. https://doi.org/10.5281/zenodo.1197110.

Ion, I., Lupu, S., 1962. Contribuţii la studiul geomorfologic al peşterii Muierilor. Analele Univ. din Bucureşti 31, 133–153.

Isola, I., Ribolini, A., Zanchetta, G., Bini, M., Regattieri, E., Drysdale, R.N., Hellstrom, J. C., Bajo, P., Montagna, P., 2019. Speleothem U /Th age constraints for the Last Glacial conditions in the Apuan Alps, northwestern Italy Palaeogeography, Palaeoclimatology, Palaeoecology Speleothem U /Th age constraints for the Last Glacial conditions in the Apuan Alps, northwestern Italy. Palaeogeogr. Palaeoclimatol. Palaeoecol. 518, 62–71. https://doi.org/10.1016/j.palaeo.2019.01.001.

Kuhlemann, J., Dobre, F., Urdea, P., Krumre, I., Gachev, E., Kubik, P., Rahn, M., 2013. Last glacial maximum glaciation of the Central South Carpathian Range (Romania). Austrian J. Earth Sci. 106, 83–95.

Lisiecki, L.E., Raymo, M.E., 2005. A Pliocene-Pleistocene stack of 57 globally distributed benthic $\delta^{18}O$ records. Paleoceanography and Paleoclimatology. 20 (1), PA1003 https://doi.org/10.1029/2004PA001071.

Longin, R., 1971. New Method of Collagen Extraction for Radiocarbon Dating. Nature 230, 241–242. https://doi.org/10.1038/230241a0.

Lyman, R.L., 1994. Vertebrate Taphonomy, Cambridge Manuals in Archaeology. Cambridge University Press, Cambridge. https://doi.org/10.1017/CBO9781139878302.

Lyman, R.L., 2017. Paleoenvironmental Reconstruction from Faunal remains: Ecological Basics and Analytical Assumptions. J. Archaeol. Res. 25, 315–371. https://doi.org/10.1007/s10814-017-9102-6.

McDermott, F., 2004. Palaeo-climate reconstruction from stable isotope variations in speleothems: a review. Quat. Sci. Rev. 23, 901–918. https://doi.org/10.1016/j.quascirev.2003.06.021.

Menot, G., Bard, E., Rostek, F., Weijers, J.W.H., Hopmans, E.C., Schouten, S., Damste, J. S.S., 2006. Early Reactivation of European Rivers during the last Deglaciation. Science (80-.) 313, 1623–1625. https://doi.org/10.1126/science.1130511.

Moldovan, O.T., Constantin, S., Panaiotu, C., Roban, R.D., Frenzel, P., Miko, L., 2016. Fossil invertebrates records in cave sediments and paleoenvironmental assessments - a study of four cave sites from Romanian Carpathians. Biogeosciences 13, 483–497. https://doi.org/10.5194/bg-13-483-2016.

Nicolăescu-Plopșor, C., 1957. Santierul arheologic Baia de Fier. Materiale și Cercetări Arheol. 3, 13–27.

Obreht, I., Hambach, U., Veres, D., Zeeden, C., Bösken, J., Stevens, T., Marković, S.B., Klasen, N., Brill, D., Burow, C., Lehmkuhl, F., 2017. Shift of large-scale atmospheric systems over Europe during late MIS 3 and implications for Modern Human dispersal. Sci. Rep. 7, 5848. https://doi.org/10.1038/s41598-017-06285-x.

Onac, B.P., Constantin, S., Lundberg, J., Lauritzen, S.E., 2002. Isotopic climate record in a Holocene stalagmite from Ursilor Cave (Romania). J. Quat. Sci. 17, 319–327. https://doi.org/10.1002/jqs.685.

Panaiotu, C., Constantin, S., Petrea, C., Horoi, V., Panaiotu, C.-E., 2013. Rock magnetic Data of late Pleistocene sediments from the Pestera cu Oase and their Paleoclimatic significance. In: Trinkaus, E., Constantin, S., Zilhão, J. (Eds.), Life and Death at the Pestera cu Oase. A Setting for Modern Human Emergence in Europe. Oxford University Press, pp. 86–99.

Parmalee, P.W., 2005. Ice Age cave faunas of North America. Geoarchaeology 20, 331–334. https://doi.org/10.1002/gea.20047.

Păunescu, A., 2001. Paleoliticul şi mezoliticul din spaţiul transilvan. Editura AGIR, Bucureşti, 574 p.

Păunescu, A., Rădulescu, C., Samson, P., 1982. Découvertes du paléolithique inférieur en Roumanie. Trav. L'Institut Speol. "Emile Racovitza" XXI, pp. 53–62.

Piotrowska, N., Goslar, T., 2002. Preparation of Bone Samples in the Gliwice Radiocarbon Laboratory for AMS Radiocarbon Dating. Isot. Environ. Health Stud. 38, 267–275. https://doi.org/10.1080/10256010208033272.

Pourmand, A., Tissot, F.L.H., Arienzo, M., Sharifi, A., 2014. Introducing a Comprehensive Data Reduction and uncertainty Propagation Algorithm for U/Th Geochronometry with Extraction Chromatography and Isotope Dilution MC-ICP-MS. Geostand. Geoanalytical Res. 38, 129–148. https://doi.org/10.1111/j.1751-908X.2013.00266.x.

Quilès, J., Petrea, C., Moldovan, O., Zilhão, J., Rodrigo, R., Rougier, H., Constantin, S., Milota, Ştefan, Gherase, M., Sarcină, L., Trinkaus, E., 2006. Cave bears (*Ursus spelaeus*) from the Peştera cu Oase (Banat, Romania): Paleobiology and taphonomy. Comptes Rendus - Palevol 5, 927–934. https://doi.org/10.1016/j.crpv.2006.09.005.

Rasmussen, S.O., Bigler, M., Blockley, S.P., Blunier, T., Buchardt, S.L., Clausen, H.B., Cvijanovic, I., Dahl-Jensen, D., Johnsen, S.J., Fischer, H., Gkinis, V., Guillevic, M., Hoek, W.Z., Lowe, J.J., Pedro, J.B., Popp, T., Seierstad, I.K., Steffensen, J.P., Svensson, A.M., Vallelonga, P., Vinther, B.M., Walker, M.J.C., Wheatley, J.J., Winstrup, M., 2014. A stratigraphic framework for abrupt climatic changes during the last Glacial period based on three synchronized Greenland ice-core records: refining and extending the INTIMATE event stratigraphy. Quat. Sci. Rev. 106, 14–28. https://doi.org/10.1016/j.quascirev.2014.09.007.

Reimer, P., Austin, W., Bard, E., Bayliss, A., Blackwell, P., Bronk Ramsey, C., Butzin, M., Cheng, H., Edwards, R., Friedrich, M., Grootes, P., Guilderson, T., Hajdas, I., Heaton, T., Hogg, A., Hughen, K., Kromer, B., Manning, S., Muscheler, R., Palmer, J., Pearson, C., van der Plicht, J., Reimer, R., Richards, D., Scott, E., Southon, J., Turney, C., Wacker, L., Adolphi, F., Büntgen, U., Capano, M., Fahrni, S., Fogtmann-Schulz, A., Friedrich, R., Köhler, P., Kudsk, S., Miyake, F., Olsen, J., Reinig, F., Sakamoto, M., Sookdeo, A., Talamo, S., 2020. The IntCal20 Northern Hemisphere radiocarbon age calibration curve (0–55 cal kBP). Radiocarbon 62. https://doi.org/10.1017/RDC.2020.41.

Reuther, A.U., Urdea, P., Geiger, C., Ivy-Ochs, S., Niller, H.P., Kubik, P.W., Heine, K., 2007. Late Pleistocene glacial chronology of the Pietrele Valley, Retezat Mountains, Southern Carpathians constrained by 10Be exposure ages and pedological investigations. Quat. Int. 164–165, 151–169. https://doi.org/10.1016/j.quaint.2006.10.011.

Riel-Salvatore, J., Popescu, G., Barton, C.M., 2008. Standing at the gates of Europe: Human behavior and biogeography in the Southern Carpathians during the late Pleistocene. J. Anthropol. Archaeol. 27, 399–417. https://doi.org/10.1016/j.jaa.2008.02.002.

Robu, M., 2015. The Palaeontology of the Cave Bear Bone Assemblage from Urşilor Cave of Chişcău – Osteometry, Palaeoichnology, Taphonomy, and Stable Isotopes. Editura Universitară, Bucharest.

Robu, M., 2016. The assessment of the internal architecture of an MIS 3 cave bear bone assemblage. Case study: Urşilor Cave, Western Carpathians. Romania. Palaeogeogr. Palaeoclimatol. Palaeoecol. 444, 115–123. https://doi.org/10.1016/j.palaeo.2015.12.012.

Rossi, C., Bajo, P., Lozano, R.P., Hellstrom, J., 2018. Younger Dryas to early Holocene paleoclimate in Cantabria (N Spain): Constraints from speleothem Mg, annual fluorescence banding and stable isotope records. Quat. Sci. Rev. 192, 71–85. https://doi.org/10.1016/j.quascirev.2018.05.025.

Sanchi, L., Ménot, G., Bard, E., 2014. Insights into continental temperatures in the northwestern Black Sea area during the last Glacial period using branched tetraether lipids. Quat. Sci. Rev. 84, 98–108.

Sasowsky, I.D., Mylorie, J., 2007. Studies of Cave Sediments. Springer Netherlands, Dordrecht. https://doi.org/10.1007/978-1-4020-5766-3.

Soulet, G., Ménot, G., Garreta, V., Rostek, F., Zaragosi, S., Lericolais, G., Bard, E., 2011. Black Sea "Lake" reservoir age evolution since the last Glacial — Hydrologic and climatic implications. Earth Planet. Sci. Lett. 308, 245–258. https://doi.org/10.1016/j.epsl.2011.06.002.

Staubwasser, M., Drăguşin, V., Onac, B.P., Assonov, S., Ersek, V., Hoffmann, D.L., Veres, D., 2018. Impact of climate change on the transition of Neanderthals to modern humans in Europe. Proc. Natl. Acad. Sci. 115, 9116–9121. https://doi.org/10.1073/pnas.1808647115.

Sun, L., Deng, C., Wang, W., Liu, C., Kong, Y., Wu, B., Liu, S., Ge, J., Qin, H., Zhu, R., 2017. Magnetostratigraphy of Plio–Pleistocene fossiliferous cave sediments in the Bubing Basin, southern China. Quat. Geochronol. 37, 68–81. https://doi.org/10.1016/j.quageo.2016.09.007.

Tămaş, T., Onac, B., Bojar, A., 2005. Lateglacial-Middle Holocene stable isotope records in two coeval stalagmites from the Bihor Mountains. NW Romania 49, 185–194.

Tîrlă, L., Drăguşin, V., Bajo, P., Covaliov, S., Cruceru, N., Ersek, V., Hanganu, D., Hellstrom, J., Hoffmann, D., Mirea, I., Sava, T., Sava, G., Şandric, I., 2020. Quaternary environmental evolution in the South Carpathians reconstructed from glaciokarst geomorphology and sedimentary archives. Geomorphology 354, 107038. https://doi.org/10.1016/j.geomorph.2020.107038.

Urdea, P., 2004. The Pleistocene glaciation of the Romanian Carpathians. Dev. Quat. Sci. https://doi.org/10.1016/S1571-0866(04)80080-0.

Urdea, P., Reuther, A., 2009. Some new data concerning the quaternary glaciation in the Romanian Carpathians. Geogr. Pannonica 13, 41–52. https://doi.org/10.5937/GeoPan0902041U.

Urdea, P., Onaca, A., Ardelean, F., Ardelean, M., 2011. New evidence on the quaternary glaciation in the romanian carpathians. Dev. Quat. Sci. 15, 305–322. https://doi.org/10.1016/B978-0-444-53447-7.00024-6.

White, W., 2007. Cave sediments and paleoclimate. J. Cave Karst Stud. 69, 79–93.

Winkler, T.S., van Hengstum, P.J., Horgan, M.C., Donnelly, J.P., Reibenspies, J.H., 2016. Detrital cave sediments record late Quaternary hydrologic and climatic variability in northwestern Florida. USA. Sediment. Geol. 335, 51–65. https://doi.org/10.1016/j.sedgeo.2016.01.022.

Zander, A., Hilgers, A., 2013. Potential and limits of OSL, TT-OSL, IRSL and pIRIR290 dating methods applied on a Middle Pleistocene sediment record of Lake El'gygytgyn, Russia. Clim. Past 9, 719–733. https://doi.org/10.5194/cp-9-719-2013.